

Role of Sigma-1 Receptor C-terminal Segment in Inositol 1,4,5-Trisphosphate Receptor Activation

CONSTITUTIVE ENHANCEMENT OF CALCIUM SIGNALING IN MCF-7 TUMOR CELLS*

Received for publication, March 17, 2008, and in revised form, June 6, 2008 Published, JBC Papers in Press, June 6, 2008, DOI 10.1074/jbc.M802099200

Zhiping Wu and Wayne D. Bowen¹

From the Department of Molecular Pharmacology, Physiology and Biotechnology, Division of Biology and Medicine, Brown University, Providence, Rhode Island 02912

Sigma-1 receptor (sigma-1R) agonists enhance inositol 1,4,5-trisphosphate (IP₃)-dependent calcium release from endoplasmic reticulum by inducing dissociation of ankyrin B 220 (ANK 220) from the IP₃ receptor (IP₃R-3), releasing it from inhibition. MCF-7 breast tumor cells express little or no sigma-1R and were used here to investigate the effect of receptor overexpression and the role of its N- and C-terminal segments in function. We stably expressed intact sigma-1R (amino acids (aa) 1–223; lines 11 and 41), N-fragment (aa 1–100; line K3), or C-fragment (aa 102–223; line sg101). C-fragment expressed as a peripheral membrane-bound protein that was removable from the endoplasmic reticulum membrane by chaotropic salt wash, consistent with lack of a putative transmembrane domain. The expressed sigma-1R, N-fragment, and C-fragment exhibited normal, low affinity, and no [³H](+)-pentazocine binding activity, respectively. All transfected lines showed constitutive enhancement of bradykinin (BDK)-induced calcium release, because of a decrease in BDK ED₅₀ values. Interestingly, sigma-1R and C-fragment had high activities, whereas the N-fragment was much less active. The antagonist BD1063 behaved as an inverse agonist in sigma-1R cells, whereas C-fragment was insensitive to ligand regulation. Like BDK, vasopressin- and ATP-induced calcium release was enhanced with the same pattern in cell lines. Anti-IP₃R-3 immunoprecipitates from cells expressing sigma-1R or C-fragment contained significantly less ANK 220 compared with untransfected or N-fragment cells, indicating a higher amount of ankyrin-free IP₃R-3. Anti-ankyrin B immunoprecipitates contained sigma-1R or C-fragment, with markedly lower levels of N-fragment present. These results suggest that sigma-1R overexpression drives sigma agonist-independent dissociation of ANK 220 from IP₃R-3, resulting in activation. The C-terminal segment plays a key role in the interaction.

Sigma receptors comprise a unique, pharmacologically defined family of proteins that bind psychotropic agents from a variety of structural classes (1–5). Sigma receptors are not only

expressed in the brain and central nervous system, but are also expressed in peripheral tissues, including liver, kidney, heart, gut, and tissues of the immune and endocrine systems (6). They are also highly expressed in tumor cell lines derived from various tissues (7). Sigma receptors have thus far been divided into sigma-1 and sigma-2 subtypes (4, 8, 9). They are noted for having high affinities for haloperidol and other typical antipsychotic agents, but they can be distinguished pharmacologically by differential affinity for dextrorotary benzomorphans, with sigma-1 receptors having high affinity and sigma-2 receptors having low to negligible affinity for these compounds (8, 9). Sigma-1 receptors are 25-kDa proteins that have been cloned and are distant homologs to the sterol isomerase enzyme of yeast and other fungi (10). Although lacking enzymatic activity, sigma-1 receptors share some pharmacology with this enzyme. No endogenous ligands have been conclusively demonstrated for sigma receptors. However, there is significant evidence that such substances exist and that they may be related to sterols (2).

Calcium ion (Ca²⁺) serves as an important intracellular signal for myriad cellular processes such as proliferation and differentiation, regulation of gene expression, and cellular stimulus-secretion coupling (11, 12). It is also known that calcium ion is toxic to cells and is involved in the triggering of events leading to apoptosis in various cell types (13, 14). Therefore, a coordinated control of the processes that alter the cytosolic free Ca²⁺ concentration ([Ca²⁺]_i)² is necessary to maintain cellular Ca²⁺ homeostasis. Ca²⁺ can be released from intracellular storage pools by certain signals such as electrical stimulation in the sarcoplasmic reticulum and by activation of inositol 1,4,5-trisphosphate (IP₃) receptors in the endoplasmic reticulum. Stimulation of G protein-coupled hormone or neurotransmitter receptors activates phospholipase-C, which catalyzes production of IP₃ and diacylglycerol. IP₃ binds to IP₃ receptors (IP₃R) and mediates Ca²⁺ release from the intracellular Ca²⁺ stores in endoplasmic reticulum (11, 12, 15). The IP₃R is regulated by a vast number of interacting proteins, including calmodulin, CaBP1, kinases, phosphatases, and components of the cytoskeleton (16).

* This work was supported by a 2007 Salomon award (to W. D. B.). The costs of publication of this article were defrayed in part by the payment of page charges. This article must therefore be hereby marked "advertisement" in accordance with 18 U.S.C. Section 1734 solely to indicate this fact.

¹ To whom correspondence should be addressed: Dept. of Molecular Pharmacology, Physiology, and Biotechnology, Box G-B389, Division of Biology and Medicine, Brown University, Providence, RI 02912. Tel.: 401-863-3253; Fax: 401-863-1595; E-mail: Wayne_Bowen@brown.edu.

² The abbreviations used are: [Ca²⁺]_i, cytosolic free Ca²⁺ concentration; IP₃, inositol 1,4,5-trisphosphate; IP₃R, IP₃ receptors; IP₃R-1, IP₃ receptor type 1; IP₃R-3, IP₃R type 3; ANK, ankyrin B; BDK, bradykinin; PTZ, (+)-pentazocine; empty vector, pcDNA3.1(–) vector without insertions; BD1063, 1-[2-(3,4-dichlorophenyl)ethyl]-4-methylpiperazine; DMEM, Dulbecco's modified Eagle's medium; aa, amino acid; ER, endoplasmic reticulum; PBS, phosphate-buffered saline; SBDL, steroid binding domain-like; GPCR, G protein-coupled receptors; RT, reverse transcription.

TABLE 1

Primers used for amplifying wild-type or truncated DNA sequences of the human sigma-1 receptor

To construct 11, 41, sg101 and K3 DNA sequences, vector of the human sigma-1 DNA sequence from ATCC was amplified by PCR using the specific 5'- and 3'-primers of sigma-1 receptor sequence shown in the table. PCR was run as described under "Experimental Procedures." The PCR amplification products were purified, digested with XhoI and BamHI, and separated by electrophoresis on 1% agarose gel. The DNA was isolated from the gel bands and ligated with the purified XhoI- and BamHI-digested pcDNA3.1(−) vector in the sense orientation. Competent *E. coli* were transformed with the constructs above and the vectors amplified. The inserted parts of the plasmids were sequenced to verify that the copies of the target sigma-1 DNA sequences were completely identical to those in the GenBank™ data base for the given segment of the receptor. For the 5'-primer, the XhoI cut site and start code are shown in underlined bold text and underlined text, respectively. The Kozak modification is shown in bold text for lines 41 and K3. For the 3'-primer, the BamHI cut site is underlined and stop code is italicized.

Cell line	5'-Primer	3'-Primer
11	5'-GCCCCTCGAGATGTCAGTGGGCCGTG3'	5'-GCCTGGATCCTCAAGGGTCCTGGCCAAAG3'
41	5'-GCCCCTCGAGATGTCAGTGGGCCGTG3'	5'-GCCTGGATCCTCAAGGGTCCTGGCCAAAG3'
K3	5'-GCCCCTCGAGATGTCAGTGGGCCGTG3'	5'-GCCTGGATCCTCACAGCGAGGCGTGCAGAAG3'
sg101	5'-GCCACTCGAGATGTCAGTATGTGCTGCTCTTCG3'	5'-GCCTGGATCCTCAAGGGTCCTGGCCAAAG3'

Several lines of evidence have shown that sigma receptors are involved in the regulation of $[Ca^{2+}]_i$. Sigma ligands from various structural classes produce a dual modulation of $[Ca^{2+}]_i$ as follows: release of Ca^{2+} from intracellular stores and blockade of depolarization-dependent influx of Ca^{2+} (17–19). Sigma-1 receptor ligands affect intrasynaptosomal free Ca^{2+} levels and protein phosphorylation in rat brain (20). Exposure of cardiac myocytes to sigma ligands was found to affect contractility, Ca^{2+} influx, and beating rate (21).

Ankyrins are a family of membrane adaptor proteins required for the localization of diverse ion channels, transporters, calcium-release channels, and cell adhesion molecules to specialized membrane domains (22). The ankyrin family is composed of ankyrin R, ankyrin B, and ankyrin G. Ankyrin B is required for the localization of the IP₃ receptor, Na^+/Ca^{2+} exchanger, and Na/K-ATPase to transverse-tubule/sarcoplasmic reticulum membranes in heart (23). Ankyrin has high affinity binding to the C terminus of IP₃R, with a K_d of 0.2 nM. The binding of ankyrin inhibits IP₃ binding and IP₃-induced internal Ca^{2+} release (24, 25). The sigma-1 receptor was found to form a trimeric complex with ankyrin B and IP₃R type 3 (IP₃R-3) in NG-108-15 neuroblastoma x glioma hybrid cells (26). Sigma-1 agonists such as (+)-pentazocine and PRE-084 caused the dissociation of an ankyrin B isoform (ankyrin B 220) from IP₃R-3, thus relieving the IP₃R inhibition and enhancing calcium release induced by a given concentration of bradykinin (BDK), a phosphoinositide agonist that generates IP₃ in these cells (26). This was blocked by a sigma-1 antagonist, which correlates excellently with mediation by sigma-1 receptors (26). However, little is known about the molecular architecture of the trimeric complex of sigma-1 receptor, ankyrin B, and IP₃R-3.

Aydar *et al.* (27) recently proposed a model for the sigma-1 receptor that includes two transmembrane domains, an extracellular loop, and intracellular N and C termini with the C-terminal region being a large soluble domain. The second transmembrane domain and the putative cytoplasmic C-terminal domain contain residues important for binding of the agonist (+)-pentazocine (28). Based on this structural model, we are investigating the functional domains of the sigma-1 receptor by making deletions of large segments of the receptor, transfecting cells to create stably expressing lines, and subsequently probing the ability of sigma-1 agonists and antagonists to modulate BDK-induced calcium release. Human MCF-7 breast tumor cells do not normally express sigma-1 receptors or express at very low levels but do express BDK receptors coupled to phos-

phoinositide turnover (7, 29, 30). Therefore, we used this as a model system in which to investigate sigma-1 receptor structure-function relationships. We made two deletion constructs where the C-terminal portion or the N-terminal portion was deleted, and we compared the function of these constructs to that of the wild-type sigma-1 receptor.

EXPERIMENTAL PROCEDURES

Construction of Expression Vectors Harboring Intact Sigma-1 Receptor or Truncated Sequences—All sequences were for the human sigma-1 receptor (GenBank™ accession number BC004899.2). Two constructs were used for the intact sigma-1 receptor. Construct 11 (to produce cell line 11) is the wild-type sequence identical to the human sigma-1 sequence (aa 1–223). Construct 41 (to produce cell line 41) is the wild-type sequence with a Kozak modification for enhanced expression, where glutamine at position 2 is replaced by glutamic acid (31). Two deletion constructs were used. Construct K3 (to produce cell line K3) is an N-terminal construct, containing the Kozak modification and with the C-terminal region deleted (aa 1–100). Construct sg101 (to produce cell line sg101) is a C-terminal construct with the N-terminal region deleted (aa 102–223). The predicted topographies of the products of the constructs are shown schematically in Fig. 1, based on the model of Aydar *et al.* (27).

Vectors containing the human sigma-1 DNA sequence were purchased from ATCC (catalog number MGC-3851). Sigma-1 DNA sequences were amplified by PCR (iCycler, Bio-Rad) using the specific 5'- and 3'-primers of sigma-1 receptor sequence shown in Table 1. PCR was run using 1 μ l of *Pfu* polymerase (Stratagene), 10 pmol of the appropriate 5'- and 3'-primers, 1 μ l of dNTPs (10 mM for each nucleotide) in a final volume of 50 μ l of regular buffer reaction mixture under the following conditions: preincubation at 94 °C for 4 min, run for 30 cycles at 94 °C for 45 s, 55 °C for 1 min, and 68 °C for 1 min, extension at 68 °C for 10 min. The PCR amplification products were purified using a PCR purification kit (Qiagen), digested with XhoI and BamHI (New England Biolabs), and separated by electrophoresis on 1% agarose gel. The DNA was isolated from the gel bands using a gel extraction kit (Qiagen). The digested DNA segments were ligated with the purified XhoI- and BamHI-digested pcDNA3.1(−) vector (Invitrogen) in the sense orientation. One Shot® Top10 chemically competent *Escherichia coli* cells (Invitrogen) were transformed with the constructs described above and the vectors amplified. The inserted parts of the plasmids were sequenced to verify that the copies of

Sigma-1 Receptor C-terminal Segment Activates IP₃ Receptor

the target sigma-1 DNA sequences were completely identical to those in the GenBankTM data base for the given segment of the receptor.

Cell Culturing and Production of Stably Transfected Cell Lines—Human MCF-7 breast tumor cells (ATCC, Manassas, VA) were cultured in Dulbecco's minimal essential medium (DMEM) containing 1.5 g/liter NaHCO₃, 10% fetal bovine serum, insulin (10 mg/liter), and penicillin/streptomycin (100 units/100 µg/ml). All cell culture processes were carried out in a humidified atmosphere of 5% CO₂, 95% air at 37 °C. To develop stably expressing cell lines, cells were plated at a density of 3×10^3 cells in 3 ml of growth medium in 35 × 10-mm Petri dishes, without antibiotics, and incubated overnight. Cells were then transfected overnight with 2.4 µg of the linearized pcDNA3.1(−) vector containing the target sigma-1 DNA sequence, as per standard protocol using LipofectamineTM (Invitrogen) in Opti-MEM[®] I medium without serum (Invitrogen). Vector-expressing cells were selected using geneticin by the following procedure. After transfection, cells were placed in normal DMEM growth medium. After 3 days, cells were detached with trypsin and replated into DMEM containing geneticin (350 µg/ml) and cultured for 25 days. Surviving cell clones were picked out and propagated separately in 35-mm dishes in the same medium, with 175 µg/ml geneticin. To suppress reversion of the phenotype, all subsequent cell culture was carried out in DMEM as described above, supplemented with 175 µg/ml geneticin.

Screening Transfected Cell Lines for Expression of Target Sigma-1 Receptor Sequences—Total RNA was extracted from cells by the guanidinium thiocyanate method (32). Quality was controlled by running 1 µg on a 1% agarose-formaldehyde gel.

Two µg of DNA-free total RNA, together with 10 pmol of 3'-primer complementary to parts of sigma-1 DNA sequence (5'-GCCTGGATCCTCAAGGGTCCTGGCCAAAG-3' for mRNA derived from cell lines 11, 41, and sg101; 5'-AGCGAG-GCGTGCAGAAG-3' for that from cell line K3) in a 12-µl volume was denatured at 70 °C for 10 min and then chilled on ice for 2 min. Two µl of first-strand buffer, 0.1 µl of 0.1 M dithiothreitol, 1 µl of 25 mM MgCl₂, and 1 µl of dNTPs were added. Transcription was started by adding 1 µl of reverse transcriptase (SuperScriptTM II, Invitrogen) per reaction, and the reaction mixture was incubated at 42 °C for 5 min and then 50 °C for 45 min. Finally, the reaction was inactivated by heating samples to 70 °C for 15 min. For PCR, 2 µl of reverse-transcribed cDNA and 1 µl of dNTPs (10 mM for each nucleotide) were added to 47 µl of conventional buffer mixture containing 10 pmol of the appropriate 5' and 3' cDNA primers as shown in Table 2, and 1 unit of *Taq* polymerase (Promega). PCR was carried out by iCycler (Bio-Rad) as follows: preincubate at 94 °C for 4 min, run for 30 cycles at 94 °C for 45 s, 55 °C for 1 min, and 72 °C for 1 min, extension at 72 °C for 10 min. Ten µl of each PCR were separated on a 1.5% agarose gel. Bands were visualized under ultraviolet light.

Western Blot Analysis of Sigma-1 Receptor Expression—Cells were grown to 90–95% confluency and washed twice with 1 × PBS buffer and dispersed with cell dissociation solution (10 ml/150-cm² flask; Sigma) at 37 °C for 25 min. Cells were then harvested by centrifuging, then resuspended with cold 1 × PBS

buffer, and harvested again. The supernatant was removed, and 0.5 ml of CellLyticTM cell lysis reagent (Sigma) per flask was added. The cells were homogenized by probe sonication for 3–5 s in an ice bath. The homogenate was centrifuged at $14,515 \times g$ at 4 °C for 20 min. The supernatant was collected and stored at −80 °C until use. Protein was determined using BCA assay (Pierce).

About 30 µg of total proteins was loaded on duplicate 15% SDS-polyacrylamide gels and subsequently blotted to a polyvinylidene difluoride membrane. Following blocking in 5% milk in PBS-T buffer (PBS with 0.2% Tween 20) for 2 h, each blot was incubated with one of the following two goat polyclonal anti-sigma receptor antibodies for 2.5 h. Goat anti-sigma-1 receptor antibody directed against a C-terminal epitope was used to probe for the intact sigma-1 receptor and the C-terminal fragment (Santa Cruz Biotechnology S-18; epitope within aa 140–200). This antibody was used at dilution 1:1000 to detect intact sigma-1 receptor and 1:100 to detect the C-terminal fragment. Goat anti-sigma-1 receptor antibody directed against an N-terminal epitope was used to probe for the N-terminal fragment (Santa Cruz Biotechnology L-20; epitope within aa 50–100). This antibody was used at dilution 1:200.

The blot was then washed with PBS-T buffer briefly and incubated with a donkey anti-goat IgG horseradish peroxidase conjugate (Santa Cruz Biotechnology) for 40 min. The Super-Signal West Pico chemiluminescent substrate kit (Pierce) was used to visualize the stained sigma-1 receptor using a Kodak Image Station 2000R. The bands were compared with protein markers of known molecular size run in parallel on the same SDS-polyacrylamide gel (Bio-Rad).

Immunoprecipitation—Cells were cultured and harvested as described above and then homogenized in an ice bath by probe sonication for 3–5 s in 500 µl 1% Triton X-100 in IP buffer (100 mM NaCl, 10 mM Tris, 5 mM EDTA (pH 7.4)) with a proteinase inhibitor mixture (CytoSignal, Irvine, CA). The homogenate was spun twice at $14,515 \times g$ for 15 min at 4 °C in microtubes, and the supernatant was removed and split into two 100- and 400-µl portions. Mouse anti-ankyrin B antibody or anti-IP₃R-3 antibody (5 µg) (Pharmingen) was added to the 400-µl sample but not to the 100-µl sample (preimmunoprecipitate). Samples were incubated for 18 h at 4 °C with gentle rocking. The immunoprecipitation was processed using an IMMUNOCatcher kit (CytoSignal, Irvine, CA). The immunoprecipitate and the preimmunoprecipitate samples were run on duplicate 15% SDS-polyacrylamide gels and subsequently blotted to a polyvinylidene difluoride membrane.

The blots were analyzed by the same procedure described above, except using a mouse anti-IP₃R type 3 antibody (1:800) or mouse anti-ankyrin B antibody (1:150) (BD Pharmingen, San Diego, CA), on the anti-IP₃R-3 immunoprecipitate. On the anti-ankyrin B immunoprecipitate, one of the two anti-sigma-1 receptor antibodies described above was used to detect the presence of intact sigma-1 receptor and the N- and C-terminal fragments. The C-terminal antibody was used at 1:100, whereas the N-terminal antibody was used at 1:200 dilution. Rabbit pre-immune serum was omitted in the anti-ankyrin B immunoprecipitate studies to prevent masking of the sigma-1 receptor by a rabbit serum protein of similar molecular weight.

Measurement of Cytosolic Free Calcium Concentration ($[Ca^{2+}]_i$)—For $[Ca^{2+}]_i$ measurement, cells were cultured up to 90% confluency, washed with 1× PBS buffer, and dispersed with cell dissociation solution (6 ml/75-cm² flask; Sigma) for 25 min at 37 °C. Cells were then harvested by centrifuging and resuspending in normal DMEM at a density of 1×10^5 cells/ml. Cells were plated into 96-well black microplates (PerkinElmer Life Sciences) and incubated at 37 °C, 5% CO₂ overnight. Each well contained about 50,000 cells. The cells were washed twice with HBS buffer (120 mM NaCl, 5 mM KCl, 1.2 mM NaH₂PO₄, 1.2 mM MgCl₂, 1.5 mM CaCl₂, 20 mM glucose, 0.33 mM sodium pyruvate, and 10 mM HEPES-NaOH (pH 7.4)). Then the cells were incubated in HBS containing 2.5 μM Fura-2 AM (Molecular Probes) and 0.066% Pluronic F-127 (Sigma). After incubation for 1 h at 37 °C in darkness, cells were washed three times with HBS buffer. After washing, wells were supplemented with 100 μl of HBS buffer (as control or for studies without sigma ligands) or HBS containing the indicated concentration of sigma-1 ligands ((+)-pentazocine or BD1063) and allowed to incubate for 16 min before measurement.

Cytosolic free calcium ($[Ca^{2+}]_i$) measurement was made using a Victor V microplate reader (PerkinElmer Life Sciences). Two excitation wavelengths of 340 and 380 nm were used and the emission was measured at 510 nm. The 510 nm emission ratio after rapid excitation at 340 and 380 nm (emission 340/380) was calculated by Dell computer. Calcium concentrations were determined by comparison to a standard curve. The standard curve was generated by using various concentrations of Ca²⁺ in the presence of 2.5 μM Fura-2 (calcium calibration buffer kit, Molecular Probes).

Basal cell $[Ca^{2+}]_i$ was measured for 20 s without any additions. Then agonist was rapidly added by pump injector to the target final concentration, usually by injecting 5 μl to a final volume of 105 μl in the well. The resultant changes in $[Ca^{2+}]_i$ were monitored for 45 s. Basal $[Ca^{2+}]_i$ levels were 50–100 nM. Cells with basal levels >100 nM were not used for study. BDK was routinely added to a final concentration of 60 nM from a stock solution of 1.26 μM made up in 0.05% acetic acid. The final concentration of acetic acid was 0.0024% and did not affect the pH or calcium signal. Where indicated, experiments were conducted with various concentrations of BDK to establish dose-response curves.

Vasopressin was added to a final concentration of 800 nM from a stock solution of 16.8 μM prepared with sterile double distilled H₂O containing 0.025% SDS. The final concentration of SDS was 0.0012%, and injection of vehicle had no effect on calcium level. ATP was added to a final concentration of 50 μM from a stock solution of 1.05 mM prepared fresh with sterile double distilled H₂O.

Membrane Preparation and Radioligand Binding—Cells were cultured to 85–90% confluency as described above in 150-cm² flasks (Costar). Total membranes were prepared as described previously (7). Briefly, medium was removed, and cells were rinsed two times with ice-cold PBS. Cells were detached by incubation with cell dissociation solution (Sigma) at 37 °C for 25 min and pelleted. The cell pellet was resuspended in ice-cold 10 mM Tris-HCl (pH 7.4), containing 0.32 M sucrose (0.5 ml/flask), and homogenized with 15 hand-driven strokes in

a Potter-Elvehjem homogenizer (Teflon pestle). The homogenate was centrifuged at $105,000 \times g$ for 15 min at 4 °C, and the supernatant was discarded. The pellet (representing the total membrane fractions of the cell) was resuspended in ice-cold 10 mM Tris-HCl (pH 7.4) to a total protein concentration of 15–20 mg/ml, and the crude membrane preparation was aliquoted and stored at –80 °C until use. Protein was measured by the BCA assay kit (Pierce).

Sigma-1 receptors were labeled using [³H](+)-pentazocine (23.4 Ci/mmol) (PerkinElmer Life Sciences) (9, 33). Nonspecific binding was determined in the presence of 10 μM haloperidol. The indicated radioligand concentrations were prepared and incubated in 50 mM Tris-HCl (pH 8.0), with 150 μg of membrane protein in a total volume of 500 μl for 120 min at 25 °C. Binding assays were terminated by dilution with 5 ml of ice-cold 10 mM Tris-HCl (pH 7.4) and filtration through polyethylenimine (0.5%)-soaked glass fiber filters using a Brandel cell harvester (Gaithersburg, MD). Filters were then washed twice with 5 ml of ice-cold buffer. Radioactivity associated with filter-trapped membranes was quantified by scintillation counting in CytosintTM (ICN; Costa Mesa, CA) using an LS6500 Scintillation Counter (Beckman Coulter, Inc. Fullerton, CA). Binding data were analyzed using GraphPad Prism 4 (San Diego, CA) to determine K_d and B_{max} values.

Determination of Membrane Distribution and Attachment of C-terminal Fragment—The membrane distribution and mode of attachment of the C-terminal fragment expressed in line sg101 cells were determined using chaotropic salt wash. Line sg101 cells were grown, harvested, and homogenized in 10 mM Tris-HCl, 0.32 M sucrose as described above for radioligand binding experiments. The homogenate was centrifuged at $1,000 \times g$ for 15 min at 4 °C, and the pellet was discarded. The resulting supernatant was centrifuged at $37,000 \times g$ for 25 min at 4 °C, and the pellet was collected (crude plasma membrane/mitochondrial, P2 fraction). The supernatant was further centrifuged at $105,000 \times g$ for 40 min at 4 °C, to collect the microsomal fraction (crude ER fraction). The resulting $105,000 \times g$ supernatant, representing the cytosolic fraction of the cells, was saved and stored at –80 °C until use.

The crude ER membrane pellet was resuspended in ice-cold 10 mM Tris-HCl (pH 7.4) to a protein concentration of 10 mg/ml, divided in 2 aliquots of 2.0 ml each, and pelleted at $105,000 \times g$ (40 min, 4 °C). One pellet was used as untreated control. The other was treated with chaotropic agents using a method described by Sazuka *et al.* (34), as follows. The membrane pellet was resuspended in 1.0 ml of solution containing 200 mM KCl and 0.1% (w/v) sodium deoxycholate using a Teflon pestle in an Eppendorf tube. The mixture was incubated for 30 min at 20 °C by gentle rotation, and the membranes were pelleted at $105,000 \times g$ for 40 min at 4 °C. The KCl/deoxycholate supernatant was saved on ice. The packed pellet was washed three times with 1 ml of water (wash discarded), followed by resuspension in 1.0 ml of 1 M NaSCN. After incubation for 30 min at 20 °C by gentle rotation, the membranes were pelleted again at $105,000 \times g$. The NaSCN supernatant was saved and combined with the KCl/deoxycholate supernatant from above. The packed pellet was again washed with water as described above. To the pellet was added 300 μl of CellLyticTM

Sigma-1 Receptor C-terminal Segment Activates IP_3 Receptor

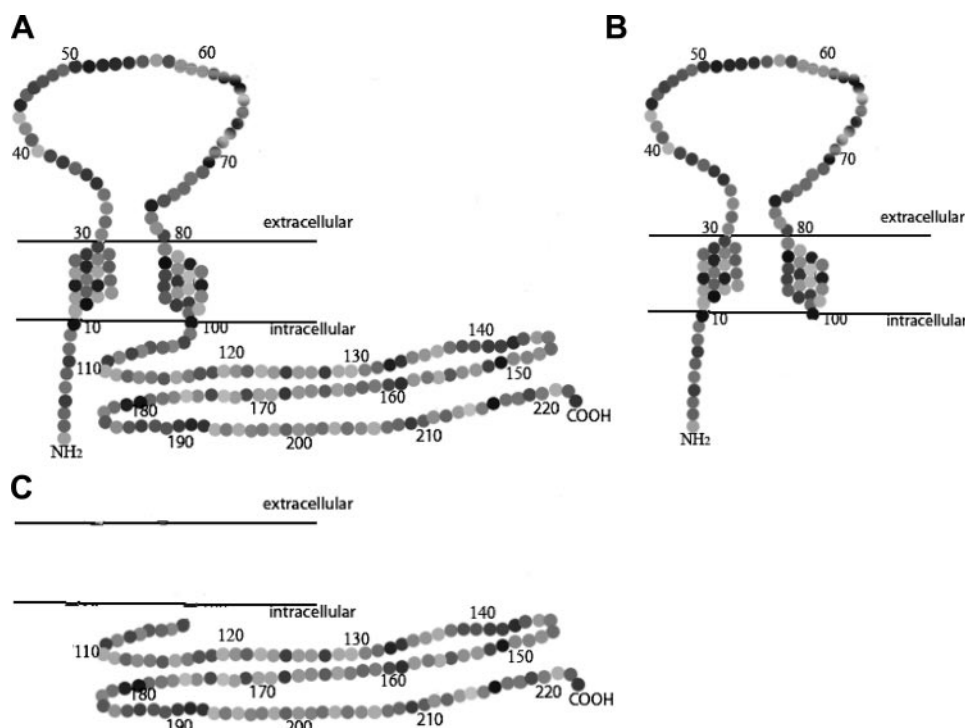


FIGURE 1. **Schematic diagrams of sigma-1 receptor constructs.** Diagram is modified from Aydar *et al.* (27). A, wild-type, aa 1–223 (cell line 11) and Kozak-modified, aa 1–223 with Gln-2 changed to Glu-2 (cell line 41); B, N-terminal construct, aa 1–100 (cell line K3); C, C-terminal construct, aa 102–223 (cell line sg101).

cell lysis reagent (Sigma). The pellets were homogenized by sonication for 3–5 s in an ice bath and allowed to stand on ice for 1 h. The homogenate was centrifuged at $14,515 \times g$ in a microcentrifuge for 20 min at 4°C and any pellet discarded. The supernatant was collected, assayed for protein, and stored at -80°C until use.

The combined KCl/deoxycholate and NaSCN supernatants from the salt treatments from the above spins were concentrated to dryness by speed-vac. The residue was reconstituted into 300 μl of CellLyticTM cell lysis reagent, assayed for protein, and stored at -80°C until further use.

For the untreated control sample, the packed membrane pellet was washed with water and then homogenized by sonication into 300 μl of CellLyticTM cell lysis reagent. The suspension was then handled as described above for the salt-treated samples.

All of the solutions described above that were exposed to membrane pellets, including the water washes, also contained proteinase inhibitor mixture (Roche Applied Science) to control protein degradation. Protein was determined using the BCA assay (Pierce).

The samples were subjected to SDS-PAGE (15% gel) and transfer to polyvinylidene difluoride membranes for Western blotting as described above. For crude ER and cytosolic fractions, 25 μg of protein was used. Protein in the combined salt wash supernatant fractions was too low to be detected by BCA assay, so 40 μl was applied. The blots were probed with the C-terminal directed anti-sigma-1 receptor antibody to detect the presence of the C-terminal fragment. Some experiments were carried out on the crude plasma membrane/

mitochondrial (P2) fraction, with intervening centrifugations at $37,000 \times g$ for 25 min at 4°C .

RESULTS

Screening of Cell Lines for Expression of Target Sigma-1 Sequences and Proteins—To investigate sigma-1 receptor functional domains, we constructed different MCF-7 breast tumor cell lines stably expressing the complete and truncated portions of the human sigma-1 receptor. Cell lines expressing the wild-type receptor, aa 1–223, were designated lines 11 and 41. A cell line expressing a truncated N-terminal portion of the receptor containing the two putative transmembrane domains, aa 1–100, was designated line K3. A cell line expressing a truncated C-terminal portion of the receptor containing the putative intracellular segment, aa 102–223, was designated sg101. The putative membrane topographies of these constructs according to the model proposed by

Aydar *et al.* (27) are shown in Fig. 1.

To confirm expression of the target construct mRNA, total mRNA from the cells was analyzed using RT-PCR using the primers shown in Table 2. In each cell type, three types of corresponding primers were used as follows: (a) primer designed to detect total sigma-1 sequence expression (endogenous plus transfected); (b) primer designed to detect only the sequence carried on the vector, and (c) primer designed to detect only endogenously expressed sequence. In each case the results were compared with a “standard” that was composed of the amplified authentic target DNA sequence. The results are shown in Fig. 2. Consistent with previous reports (7, 35, 36), MCF-7 cells showed little or no expression of endogenous sigma-1 receptors (Fig. 2A). Lines 41 and 11 showed expression of the expected complete (Kozak-modified and wild-type) sigma-1 receptor sequence, both in the total mRNA and in the vector-only pool, but no endogenously expressed sequence (Fig. 2B). Note that sigma-1 sequence expressed on the vector is shifted to a slightly higher size, indicating amplification of vector DNA sequence in addition to sigma-1 sequence. Lines K3 and sg101 both expressed the expected truncated transcripts, with neither expressing any endogenous truncated sequence (Fig. 2, C and D).

To confirm expression of sigma-1 receptor-related proteins, cell extracts were subjected to Western blot analysis using commercial sigma-1 receptor antibodies. These results are shown in Fig. 3. Separate sigma-1 receptor antibodies directed against an N-terminal epitope and a C-terminal epitope were used for these studies.

TABLE 2**Primers used for screening stably expressing cell lines**

Reverse-transcribed cDNA of each cell line was obtained as described under "Experimental Procedures." Conventional buffer mixture (47 μ l) containing 10 pmol of the appropriate 5' and 3' cDNA primers in the table was added with 2 μ l of the relative cDNA, 1 μ l of dNTPs (10 mM for each nucleotide) and 1 unit of *Taq* polymerase (Promega). PCR was carried out as described under "Experimental Procedures." Ten μ l of each PCR product was separated on a 1.5% agarose gel and visualized under ultraviolet light.

Target sigma-1	Cell line	5'-Primer	3'-Primer
Total wild type or truncated sigma-1	11, MCF-7	5'-GATGCAGTGGGCCGTG-3'	5'-TCAAGGGTCTGGCCAAAG-3'
	41	5'-GATGGAGTGGGCCGTG-3'	5'-TCAAGGGTCTGGCCAAAG-3'
	K3	5'-GATGGAGTGGGCCGTG-3'	5'-AGCGAGGCGTGCAGAAG-3'
	sg101	5'-GAGTATGTGCTGCTCTTCG-3'	5'-TCAAGGGTCTGGCCAAAG-3'
	41, 11, sg101, MCF-7	5'-AATACGACTCACTATAGGGAG-3'	5'-GCCTGGATCCTCAAGGGTCTGGCCAAAG-3'
Vector wild type or truncated sigma-1	K3	5'-AATACGACTCACTATAGGGAG-3'	5'-AGCGAGGCGTGCAGAAG-3'
	MCF-7, 41, 11, sg101	5'-CCTGAGCTGCGCCGTG-3'	5'-TCAAGGGTCTGGCCAAAG-3'
Endogenous wild type or truncated sigma-1	K3	5'-CCTGAGCTGCGCCGTG-3'	5'-AGCGAGGCGTGCAGAAG-3'

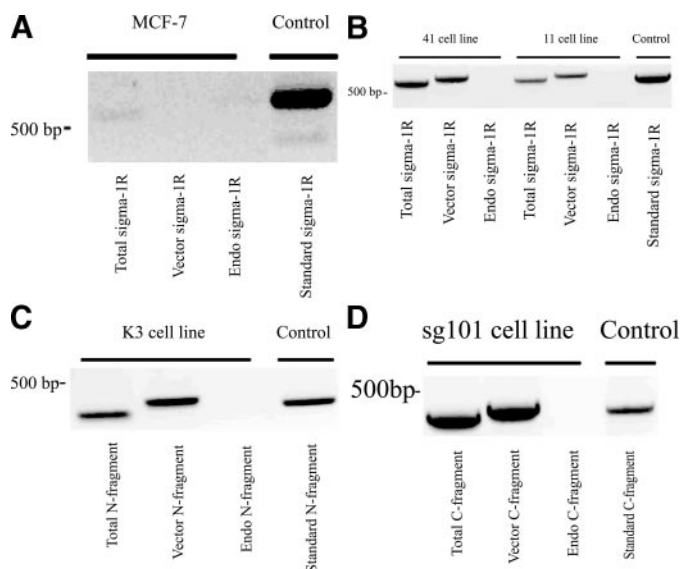


FIGURE 2. Screening of cell lines for stable expression of target sigma-1 receptor mRNA sequences. Total RNA was extracted from cells by the guanidinium thiocyanate method and reverse-transcribed as described under "Experimental Procedures." For PCR screening, 2 μ l of reverse-transcribed cDNA and 1 μ l of dNTPs were added to a conventional buffer mix containing 10 pmol of the appropriate 5' and 3' cDNA primers and 1 unit of *Taq* polymerase, and the reaction was carried out as described under "Experimental Procedures." The specific 5' and 3' cDNA primers used to amplify the individual sigma-1 receptor-related sequences are shown in Table 2. The lanes of the gels are labeled as follows: *Total* = amplification of total sigma-1-related mRNA (endogenously expressed + expression from vector); *Vector* = amplification of sigma-1-related sequence carried on the designated vector; *Endo* = detection of endogenously expressed sigma-1-related sequence; *Standard* = amplification of a standard representing the sequence in question (control sequence). *A*, sigma-1 (wild type) PCR products in MCF-7 cells. The vector used here was an empty vector control. *B*, PCR products in line 41 cells (Kozak modification) and line 11 cells (wild type). *C*, PCR products in Line K3 cells (N-terminal fragment; aa 1–100). *D*, PCR products in line sg101 cells (C-terminal fragment; aa 102–223).

The C-terminal directed antibody was used to probe for the intact sigma-1 receptor and the C-terminal fragment (Fig. 3, *A* and *B*). At an antibody dilution of 1:1000, no sigma-1 receptor was detected in untransfected MCF-7 cells (Fig. 3*A*). Intact sigma-1 receptor (25 kDa) was detected in both line 11 and line 41 cells (Fig. 3*A*). At the antibody dilution of 1:1000, sufficient to detect the expressed intact sigma-1 receptor, no C-terminal fragment product was detected in line sg101 (Fig. 3*A*). However, at a dilution of 1:100, the C-terminal fragment protein (13.7 kDa) was strongly detected in line sg101 (Fig. 3*B*).

The N-terminal directed sigma-1 antibody was used to probe for the N-terminal fragment. Using the antibody at a dilution of

1:200, the N-terminal fragment (11.4 kDa) could be detected in extracts from line K3 cells (Fig. 3*C*). Overall, these results are consistent with the PCR data, showing that all of the expected protein products are stably expressed in the cell lines. The need to use the respective antibodies at a lower dilution to detect the fragments could either indicate a lower abundance of these proteins in the cells or that the antibodies have lower affinity for the fragments compared with the intact protein.

Membrane Localization and Attachment of C-terminal Fragment in Line sg101—Based on the sigma-1 topology model of Aydar *et al.* (27) (Fig. 1), the C-terminal fragment construct expressed in line sg101 would not have a transmembrane domain. Computational analysis of the sigma-1 protein sequence predicts a short, third hydrophobic helix at the C terminus that could enable attachment to the membrane.³ Alternatively, the protein could remain free in the cytosol. Thus we investigated the membrane localization of the C-terminal fragment and its mode of attachment by determining sensitivity to salt extraction.

Line sg101 homogenates were subjected to differential centrifugation to isolate crude plasma membrane/mitochondrial (P2) and ER fractions. The ER fraction was treated with or without chaotropic agents and then subjected to Western analysis for C-terminal fragment. Fig. 3*D* shows that in untreated samples the C-terminal fragment is strongly localized to the endoplasmic reticulum membrane fraction. There was also some detection of C-terminal fragment protein in the cytosol. After treatment of the membrane fractions with 200 mM KCl, 0.1% deoxycholate, 1 M NaSCN, the level of C-terminal fragment in the ER fraction was greatly reduced, with a concomitant increase in the soluble wash fraction. The protein was also detected at a lower level in the crude plasma membrane/mitochondrial (P2) fraction, and the salt wash also reduced its content in this membrane fraction (data not shown). This suggests that the C-terminal fragment is preferentially localized to the ER membrane fraction. However, it is not strongly anchored there as an integral membrane protein but rather attached in the manner of a peripheral protein.

Characterization of Radioligand Binding Parameters of the Sigma-1 Receptor Constructs Using [³H](+)-Pentazocine—(+)-Pentazocine is a highly selective sigma-1 receptor agonist, and [³H](+)-pentazocine is a widely used selective probe to assess ligand binding characteristics of sigma-1 receptors *in vitro* (33).

³ W. Peti, unpublished observations.

Sigma-1 Receptor C-terminal Segment Activates IP₃ Receptor

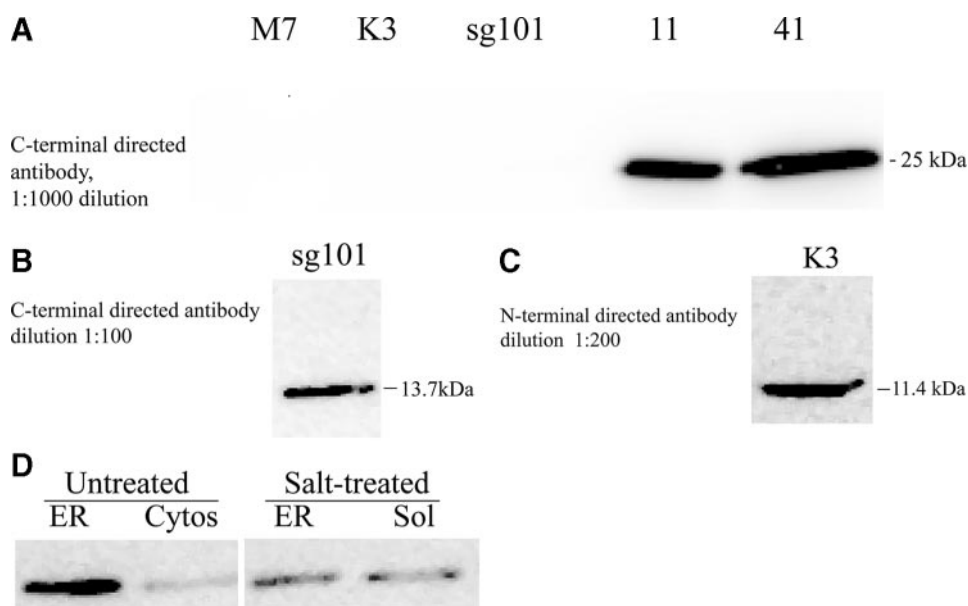


FIGURE 3. Western blot analysis of cell lines for stable expression of target sigma-1 receptor proteins. Extracts of each cell line were prepared and subjected to SDS-PAGE and Western blotting as described under "Experimental Procedures," using commercially available anti-sigma-1 receptor antibody directed at either an N-terminal or C-terminal epitope of the receptor (Santa Cruz Biotechnology). Images shown are from chemiluminescence visualization. The 10–27-kDa region of the blot is shown. *A*, C-terminal directed antibody at 1:1000 dilution, detecting 25-kDa intact sigma-1 receptor (M7 = untransfected MCF-7 cells). *B*, C-terminal directed antibody at 1:100 dilution, detecting 13.7-kDa C-terminal fragment. *C*, N-terminal directed antibody at 1:200 dilution, detecting 11.4-kDa N-terminal fragment. *D*, membrane distribution and attachment of C-terminal fragment. Line sg101 cells were homogenized and fractionated into crude plasma membrane/mitochondrial, crude microsomal, and cytosolic fractions, as described under "Experimental Procedures." The ER fraction was then treated with sequential exposure to chaotropic agents (200 mM KCl, 0.1% (w/v) sodium deoxycholate, and 1 M NaSCN) as described under "Experimental Procedures." The treated membranes and the resultant wash fraction (Sol) were subjected to Western blot analysis using a C-terminal directed anti-sigma-1 receptor antibody (1:100 dilution) and compared with untreated membranes and cell cytosol (Cytosol).

Ligand binding parameters for [³H](+)-pentazocine were determined using total membrane preparations from the cell lines. The results from saturation binding and Scatchard analysis are shown in Fig. 4 and are summarized in Table 3.

Untransfected MCF-7 cells possess a saturable [³H](+)-pentazocine-binding site with $K_d = 393$ nM and $B_{max} = 1,431$ fmol/mg protein (Fig. 4A and Table 3). This low affinity binding site is not the prototypic sigma-1 receptor, which has K_d of 3–10 nM across different tissues (33). This site is endogenously expressed. Its identity is not clear, but could represent a sigma-1 receptor splice variant (37).

Line 11 (Fig. 4B) and line 41 (Fig. 4C) both expressed saturable, high affinity [³H](+)-pentazocine-binding sites with K_d values in the normal range for sigma-1 receptors, 7.43 and 3.88 nM, respectively. The high B_{max} values of 16,710 and 31,110 fmol/mg protein confirm overexpression of wild-type sigma-1 receptor protein. The nearly 2-fold higher expression level in line 41 compared with line 11 is consistent with the Western blot data shown in Fig. 3A and with the RT-PCR data shown in Fig. 2B, where the bands from line 41 are darker than those from line 11. Furthermore, to achieve a higher expression level in line 41, a Kozak consensus sequence was engineered in the frame of the first ATG of the sigma-1 cDNA (31). The Kozak modification involves replacement of glutamine by glutamic acid at position 2 of the sigma-1 receptor sequence. The data indicate that, compared with the unmodified wild-type sequence expressed in line 11, the change has no effect on ligand binding

but does indeed lead to the desired higher expression level. It should be noted that because of the very high number of high affinity [³H](+)-pentazocine-binding sites present in these cell lines, an attempt to detect the endogenously expressed low affinity sites was not made.

Line sg101 expresses the C-terminal segment of the sigma-1 receptor (Fig. 1). This cell line exhibited only the endogenously expressed low affinity [³H](+)-pentazocine-binding site expressed in the untransfected cells (Fig. 4D). No additional [³H](+)-pentazocine-binding site could be detected, indicating that the C-terminal fragment does not bind ligand.

Line K3 expresses the N-terminal segment of the sigma-1 receptor (Fig. 1). This cell line showed two classes of binding sites for [³H](+)-pentazocine (Fig. 4E and Table 3). Site 1 represents a saturable, low affinity binding site of comparable K_d and B_{max} values to that observed in the untransfected MCF-7 cells, and likely represents the endogenously expressed site. Site 2 is a site of low affinity and high capacity that

was not saturable in the practical range of (+)-pentazocine concentrations used in these experiments (up to 1,000 nM under "hot plus cold" saturation experiments). Thus, because of the nature of this site, the binding parameters cannot accurately be determined using the current technique ($K_d > 1,000$ nM; $B_{max} > 3,000$ fmol/mg protein). However, the data do indicate that the K3 cell line expresses a protein in addition to the endogenous site, which has the ability to bind (+)-pentazocine with low affinity and this corresponds to the N-terminal sigma-1 fragment transfected into these cells.

Table 4 shows the relative level of binding at three different [³H](+)-pentazocine concentrations (110, 310, and 1010 nM) for membranes from untransfected MCF-7 cells, line sg101, and line K3. The table shows that although all three cell lines express the endogenous low affinity [³H](+)-pentazocine-binding site in comparable numbers (Table 3), the level of [³H](+)-pentazocine binding is significantly higher in K3. This indicates that the very low affinity of the N-terminal construct for (+)-pentazocine is likely compensated by a relatively high level of expression, leading to significant (+)-pentazocine binding to these membranes over reasonable concentration ranges.

Effect of Sigma Ligands on Bradykinin-stimulated Calcium Release in Untransfected MCF-7 Cells—Su and co-workers (38) used BDK-induced calcium release to demonstrate that agonist activation of sigma-1 receptors in NG-108-15 neuroblastoma-glioma hybrid cells amplifies calcium efflux from the endoplasmic reticulum by IP₃. These studies showed that pretreatment

of cells with nanomolar concentrations of sigma-1 agonists such as (+)-pentazocine, pregnenolone sulfate, and PRE-084 were without effect by themselves, but potentiated the BDK-induced increase of the cytosolic free Ca^{2+} ($[\text{Ca}^{2+}]_i$) concentration in a bell-shaped manner (38). This effect was blocked by sigma-1 receptor antagonists. MCF-7 breast tumor cells are known to express bradykinin receptors coupled to phosphoinositide turnover, IP₃ production, and calcium release from the ER (7, 29, 30). Thus, we have used BDK here to aid in examining the structure-function relationship for calcium release in untransfected MCF-7 cells and MCF-7 cells expressing the various forms of the sigma-1 receptor.

Fig. 5 shows that 60 nM BDK induces a rapid and transient calcium signal in untransfected MCF-7 cells. A 16-min pretreatment of cells with either the sigma-1 agonist (+)-pentazocine (100 nM), the antagonist BD1063 (30 μM), or the combination of (+)-pentazocine and BD1063 had no effect on the calcium signal generated by subsequent addition of BDK. The lack of effect of any sigma ligands on the BDK response is consistent with the lack of sigma-1 receptors in these cells.

Overexpression of Sigma-1 Receptor and Its Truncated Forms Potentiates BDK-induced Calcium Release in MCF-7 Cells—Fig. 6A shows the effect of 60 nM BDK on $[\text{Ca}^{2+}]_i$ in lines 11, 41, K3, and sg101 in the absence of sigma ligands, compared with untransfected MCF-7 cells and MCF-7 cells transfected with an empty vector pcDNA3.1(–). The bar graph in Fig. 6B shows the peak level of calcium reached in each of the cell lines. All of the cell lines exhibited an increase in $[\text{Ca}^{2+}]_i$ in response to addition of 60 nM BDK. Surprisingly, the response to BDK was significantly higher in all of the transfected cell lines compared with untransfected and empty vector-transfected MCF-7 cells. Line 41 cells overexpressing the Kozak-modified wild-type sigma-1 recep-

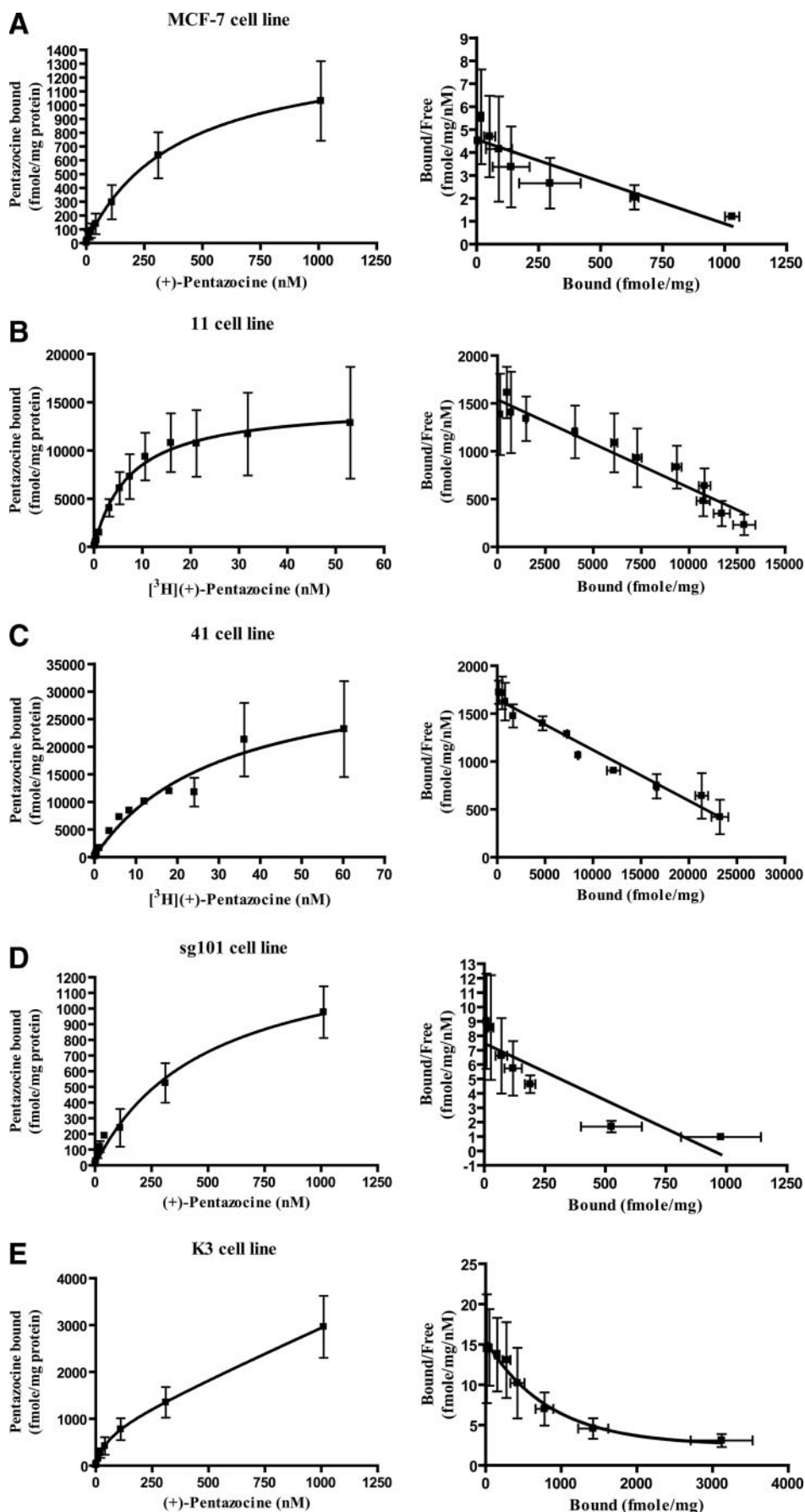


TABLE 3**Binding parameters for [³H](+)-pentazocine in transfected and untransfected MCF-7 cell lines**

Membrane preparation and radioligand binding were conducted as described under "Experimental Procedures." Binding data were analyzed using GraphPad Prism 4 to determine K_d and B_{max} values. Data are summarized from Fig. 4.

Cell line	K_d	B_{max}
	<i>nM</i>	<i>fmol/mg membrane protein</i>
MCF-7 (untransfected)	393 ± 181	1431 ± 281
11	7.43 ± 3.98	16,710 ± 4710
41	3.88 ± 2.72	31,110 ± 4480
sg101	493 ± 190	1438 ± 253
K3	207 ± 45.5 (K_{d1}) >1,000 ^a (K_{d2})	654 ± 217 (B_{max1}) >3,000 ^b (B_{max2})

^a Saturation was not achieved at maximum ligand concentration of 1,000 nM used.

^b B_{max2} represents amount bound at this subsaturating concentration.

TABLE 4**Relative levels of (+)-pentazocine binding in membranes from MCF-7, line sg101, and line K3 cells**

Binding levels of (+)-pentazocine at concentrations of 110, 310, and 1,010 nM in the three cell lines were taken from the data of Fig. 4, A, D, and E and shown in the table.

Cell line	[³ H](+)-Pentazocine binding, radioligand concentration		
	110 nM	310 nM	1010 nM
	<i>fmol/mg membrane protein</i>		
MCF-7	296 ± 124	636 ± 167	1,030 ± 289
sg101	239 ± 120	526 ± 126	978 ± 165
K3	778 ± 232	1,421 ± 398	3,119 ± 668

tor showed a 4-fold higher BDK response compared with untransfected or empty vector cells. Line 11 cells, also expressing wild-type receptor, showed a 2-fold higher response. This suggests constitutive sensitization of the BDK response and is consistent with the 2-fold difference in sigma-1 receptor expression between line 41 and line 11 (Table 3).

Most surprising is the sensitization in BDK response exhibited in line sg101, expressing only the C-terminal segment of the receptor. The BDK response in this cell line was comparable with that in line 41, which expresses the intact receptor. Line K3, expressing the N-terminal segment, also showed an enhanced BDK response relative to untransfected cells and was comparable with that of line 11. These data suggest that the truncated sigma-1 receptors are differentially able to constitutively regulate the BDK sensitivity of the cells.

To determine how the sigma-1 fragments are increasing the BDK calcium response, BDK dose-response curves were obtained in each cell line. The results are shown in Fig. 7. With the exception of line K3, BDK produced the same maximal response in all the cell lines. In untransfected MCF-7 cells, the

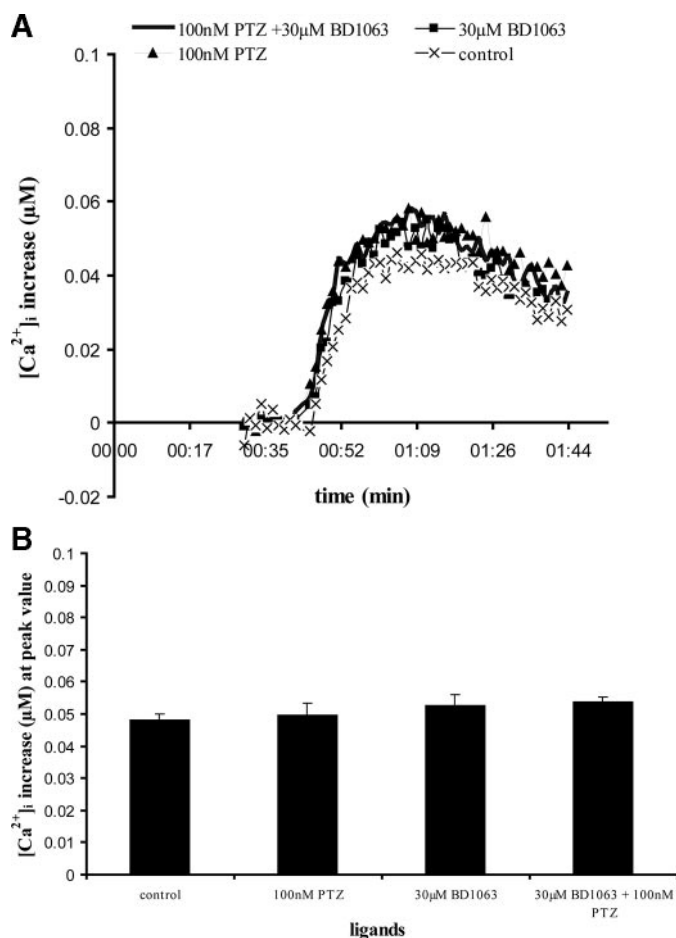


FIGURE 5. Effect of sigma ligands on BDK-induced calcium release in untransfected MCF-7 cells. MCF-7 cells were loaded with fura-2 and stimulated with 60 nM BDK with or without pretreatment with various sigma ligands, and changes in $[Ca^{2+}]_i$ were measured as described under "Experimental Procedures." The sigma ligands used were (+)-pentazocine (100 nM), BD1063 (30 μ M), and the combination of (+)-pentazocine (100 nM) and BD1063 (30 μ M). The sigma ligands were preincubated with cells for 16 min prior to rapid injection of BDK. A, representative time versus $[Ca^{2+}]_i$ traces. The individual traces were normalized by subtracting the base line. Each point is the averaged value from 6 wells. For clarity, the error bars have been removed. Standard error across the 6 wells was within 1.09%. The experiment for each curve was repeated 4–7 times with similar results. B, comparison of peak values from time versus $[Ca^{2+}]_i$ traces. Each value represents the mean of peak $[Ca^{2+}]_i$ from traces from six separate experiments, normalized relative to base line. Values shown are \pm S.E. Relative to the control pretreated with no ligands, none of the ligands produced effects significantly different from control as analyzed by Student's *t* test. $p = 0.1926$, 0.8081 , and 0.4472 for 100 nM PTZ; 30 μ M BD1063; and 100 nM PTZ + 30 μ M BD1063, respectively, relative to the control. $p < 0.05$ indicates significance.

FIGURE 4. Saturation binding and Scatchard analysis of [³H](+)-pentazocine binding to membranes from MCF-7 cells and transfected MCF-7 cell lines. A total membrane fraction was prepared from each cell line as described under "Experimental Procedures." Membranes were then incubated with [³H](+)-pentazocine under the conditions described under "Experimental Procedures" using either the "hot only" or "hot + cold" methods as indicated. Saturation isotherm (left) and Scatchard plot (right) are shown for each cell line. K_d and B_{max} values were determined by analysis using GraphPad Prism 4 (San Diego, CA). Values shown are averages of three experiments \pm S.E., each carried out in triplicate. K_d and B_{max} values in each cell line are summarized in Table 3 for convenience. A, untransfected MCF-7 cells. To obtain the full range of concentrations up to 1,000 nM, a combination of hot only and hot + cold incubations were used. Four concentrations of [³H](+)-pentazocine up to 10.3 nM were used, followed by combination of 10.3 nM [³H](+)-pentazocine with four concentrations of unlabeled (+)-pentazocine up to 1,000 nM to give a total of eight points. The data were fit to both one-site and two-site binding models. The absolute sum of squares values revealed that the models were not statistically different, thus the simplest model is used. $K_d = 393 \pm 181$ nM; $B_{max} = 1,431 \pm 281$ fmol/mg protein. B, line 11 cells. Membranes were incubated with 12 concentrations of [³H](+)-pentazocine ranging from 0.1 to 53.1 nM. $K_d = 7.43 \pm 3.98$ nM; $B_{max} = 16,710 \pm 4,710$ fmol/mg protein. C, line 41 cells. Membranes were incubated with 12 concentrations of [³H](+)-pentazocine ranging from 0.1 to 60.2 nM. $K_d = 3.88 \pm 2.72$ nM; $B_{max} = 31,110 \pm 4,480$ fmol/mg protein. D, line sg101 cells. Membranes were incubated with labeled and unlabeled (+)-pentazocine up to a concentration of 1,000 nM, as described in A above. $K_d = 493 \pm 190$ nM; $B_{max} = 1,438 \pm 253$ fmol/mg protein. E, line K3 cells. Membranes were incubated with labeled and unlabeled (+)-pentazocine up to a concentration of 1,000 nM, as described in A above. The data were best fit to a two-site model, with $K_{d1} = 207 \pm 45.5$ nM; $B_{max1} = 654 \pm 217$ fmol/mg protein and $K_{d2} = >1,000$ nM; $B_{max2} > 3,000$ fmol/mg protein.

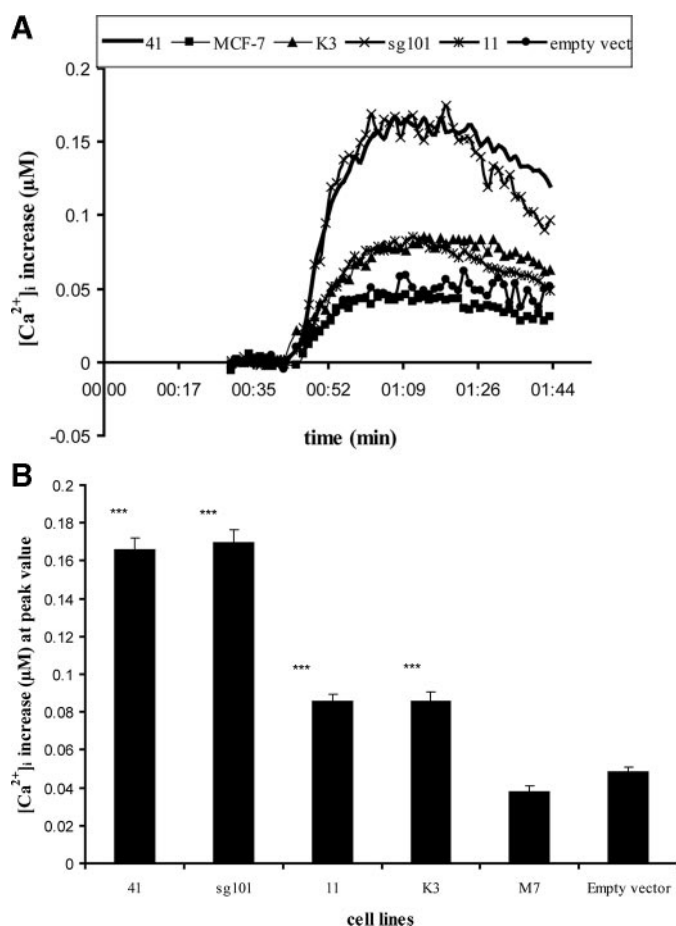


FIGURE 6. Effect of BDK on $[Ca^{2+}]_i$ in cell lines expressing the sigma-1 receptor and its truncated forms. The various cell lines were loaded with Fura-2 as described under "Experimental Procedures." After recording base line, BDK was rapidly injected to a final concentration of 60 nM, and $[Ca^{2+}]_i$ levels recorded and analyzed as described under "Experimental Procedures." **A**, representative time versus $[Ca^{2+}]_i$ traces for the different cell lines are shown, with all values normalized to base line. Each point is the averaged value from 6 wells. For clarity, the error bars have been removed. Standard error across the 6 wells was within 5.0%. Experiment was repeated six times. **B**, comparison of peak values from time versus $[Ca^{2+}]_i$ traces. Each value represents the mean of peak $[Ca^{2+}]_i$ values from six separate experiments, \pm S.E. Student's *t* test was used to analyze differences in the various transfected cell lines relative to untransfected MCF-7 cells (labeled M7). With the exception of cells transfected with empty vector, all of the constructs showed highly significant differences, relative to untransfected control: $p < 0.0001$ for 41, sg101, 11, and K3 cell lines. $p = 0.0766$ for cells transfected with empty vector. $p < 0.05$ indicates significance. Asterisks indicate a significant difference: * = $p < 0.05$; ** = $p < 0.01$; *** = $p < 0.0001$.

ED₅₀ of BDK was 85.5 nM. However, the BDK dose-response curves for lines 41, 11, and sg101 were shifted to the left relative to untransfected MCF-7 cells, with ED₅₀ values of 3.28, 12.1, and 7.4 nM, respectively. Interestingly, in line K3 the maximal response was markedly reduced relative to the other cell lines, whereas the ED₅₀ was 3.07 nM, comparable with the more active constructs. These results show that the enhanced calcium response for all of the constructs is largely because of an apparent increase in the potency of BDK, rather than an increase in maximal response.

Effect of Sigma Ligands on BDK-induced Changes in $[Ca^{2+}]_i$ in Lines 11 and 41—Fig. 8, A and B, shows the effect of sigma-1 receptor agonist and antagonist on the BDK calcium response in lines 11 and 41, respectively. The cells were pretreated with

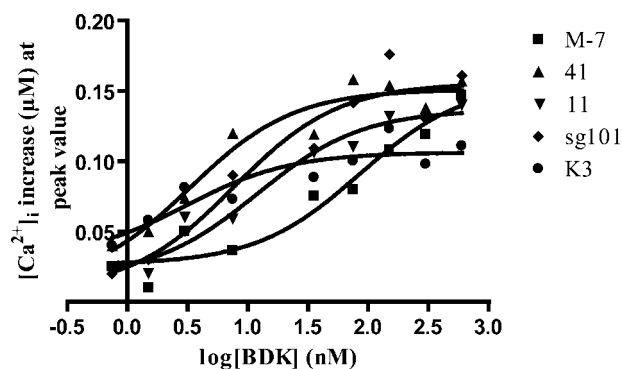


FIGURE 7. Dose-response curves for BDK-induced calcium release in untransfected and transfected MCF-7 cell lines. MCF-7 cell lines were loaded with fura-2 and stimulated with 0.75, 1.5, 3.0, 7.5, 37.5, 75, 150, 300, and 600 nM BDK (without pretreatment with any sigma ligands), and changes in $[Ca^{2+}]_i$ were measured as described under "Experimental Procedures." Values shown are the averages of data from 6 to 12 wells. Error bars are eliminated for clarity. Curves were fitted using GraphPad Prism 4 (San Diego, CA), and ED₅₀ values were determined. ED₅₀ values were as follows: untransfected MCF-7 (M-7), 85.5 nM; line 41, 3.28 nM; line 11, 12.1 nM; line sg101, 7.69 nM; and line K3, 3.07 nM. A similar maximal response was attained with all cell lines, with the exception of line K3, which exhibited a lower maximal response.

or without the indicated sigma ligand(s) for 16 min, prior to addition of 60 nM BDK to stimulate the rise in $[Ca^{2+}]_i$. Control cells were stimulated with BDK in the absence of sigma ligands. The bar graphs beside traces in Fig. 8A show the peak $[Ca^{2+}]_i$ reached. In line 11, (+)-pentazocine had a significant enhancing effect on the BDK stimulated rise in $[Ca^{2+}]_i$. However, the antagonist BD1063, when added alone, had a marked inhibitory effect on the BDK response compared with control. Combining (+)-pentazocine with BD1063 resulted in no net change upon addition of BDK, relative to control. Thus BD1063 behaved as an inverse agonist, the effect of which is blocked by addition of the agonist. These data strongly suggest that the overexpressed wild-type sigma-1 receptor is constitutively active in line 11 cells, positively modulating the release of calcium in response to BDK. Fig. 8B shows the same experiment carried out in line 41 cells. Similar results were observed as with line 11 cells.

Effect of Sigma Ligands on BDK-induced Changes in $[Ca^{2+}]_i$ in Line K3—Fig. 8C shows the effects of sigma ligands on the BDK response in line K3, expressing the N-terminal segment of the receptor. Unlike the expected effect to enhance the response, pretreatment of K3 cells with (+)-pentazocine resulted in an anomalous decrease in the BDK-induced calcium response compared with control. Thus, (+)-pentazocine behaved as an inverse agonist. Likewise, BD1063 also decreased the response. The combination of (+)-pentazocine and BD1063 resulted in a BDK response no different from the effect of either ligand alone. The results show that the constitutive enhancement effect produced by the truncated N-terminal segment of the receptor is fully modulated by sigma ligands, although in an anomalous manner where both agonist and antagonist behave as inverse agonists. This ability to be regulated by ligands is consistent with the ability of the N-terminal fragment to exhibit [³H](+)-pentazocine binding, albeit with low affinity (Fig. 4E and Tables 3 and 4).

Effect of Sigma Ligands on BDK-induced Changes in $[Ca^{2+}]_i$ in Line sg101—Fig. 8D shows the effects of sigma ligands on the BDK response in line sg101, expressing the C-terminal segment

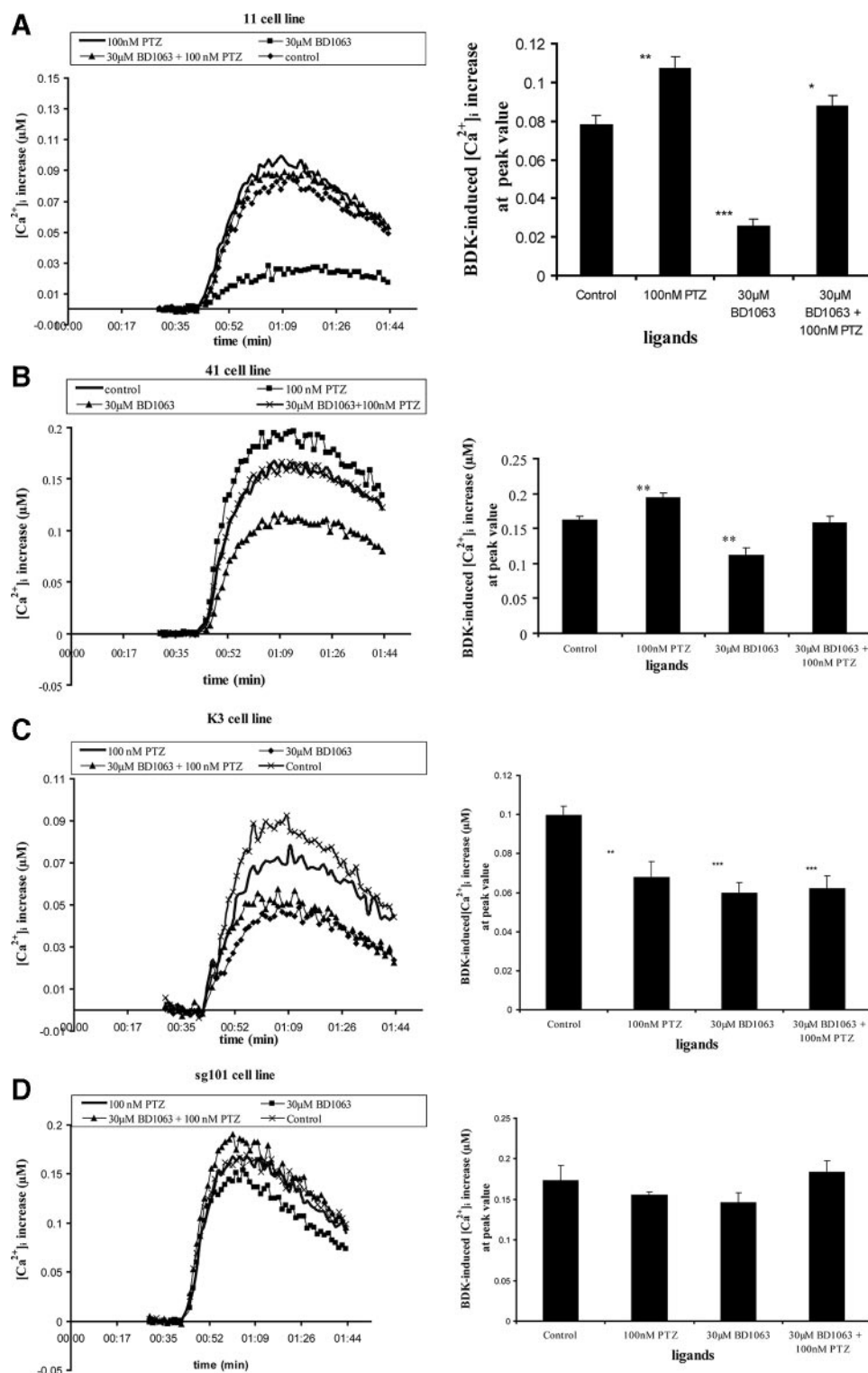


FIGURE 8. Effect of sigma ligands on BDK-induced calcium release in cell lines expressing the sigma-1 receptor and its truncated forms. Cells were loaded with Fura-2 and treated with or without sigma receptor ligands before stimulation with 60 nM BDK as described under "Experimental Procedures" and the legend of Fig. 5. Data were treated as described in the legend to Fig. 5. For each lettered panel, the graph on the left shows representative time versus $[Ca^{2+}]_i$ traces for each condition. The graph on the right is a comparison of peak values from the time versus $[Ca^{2+}]_i$ traces shown as a bar graph, with each value representing the mean of peak $[Ca^{2+}]_i$ values from six separate experiments, \pm S.E. Student's *t* test was used to analyze differences in the various conditions relative to the control (no sigma ligand). Asterisks over bars indicate a significant difference: * = $p < 0.05$; ** = $p < 0.01$; *** = $p < 0.0001$. PTZ = (+)-pentazocine. A, line 11 cells as follows: $p = 0.0058$, <0.0001 , and 0.0136 for 100 nM PTZ, 30 μ M BD1063, and 100 nM PTZ + 30 μ M BD1063, respectively, relative to the control. B, line 41 cells as follows: $p = 0.0056$, 0.0024 , and 0.7573 for 100 nM PTZ, 30 μ M BD1063, and 100 nM PTZ + 30 μ M BD1063, respectively, relative to the control. C, line K3 cells as follows: $p = 0.006$, 0.0002 , and 0.0008 for 100 nM PTZ, 30 μ M BD1063, and 100 nM PTZ + 30 μ M BD1063, respectively, relative to the control. D, line sg101 cells as follows: none of the sigma ligands had a significant effect on BDK-induced calcium changes. $p = 0.3494$, 0.2343 , and 0.6947 for 100 nM PTZ, 30 μ M BD1063, and 100 nM PTZ + 30 μ M BD1063, respectively, relative to the control.

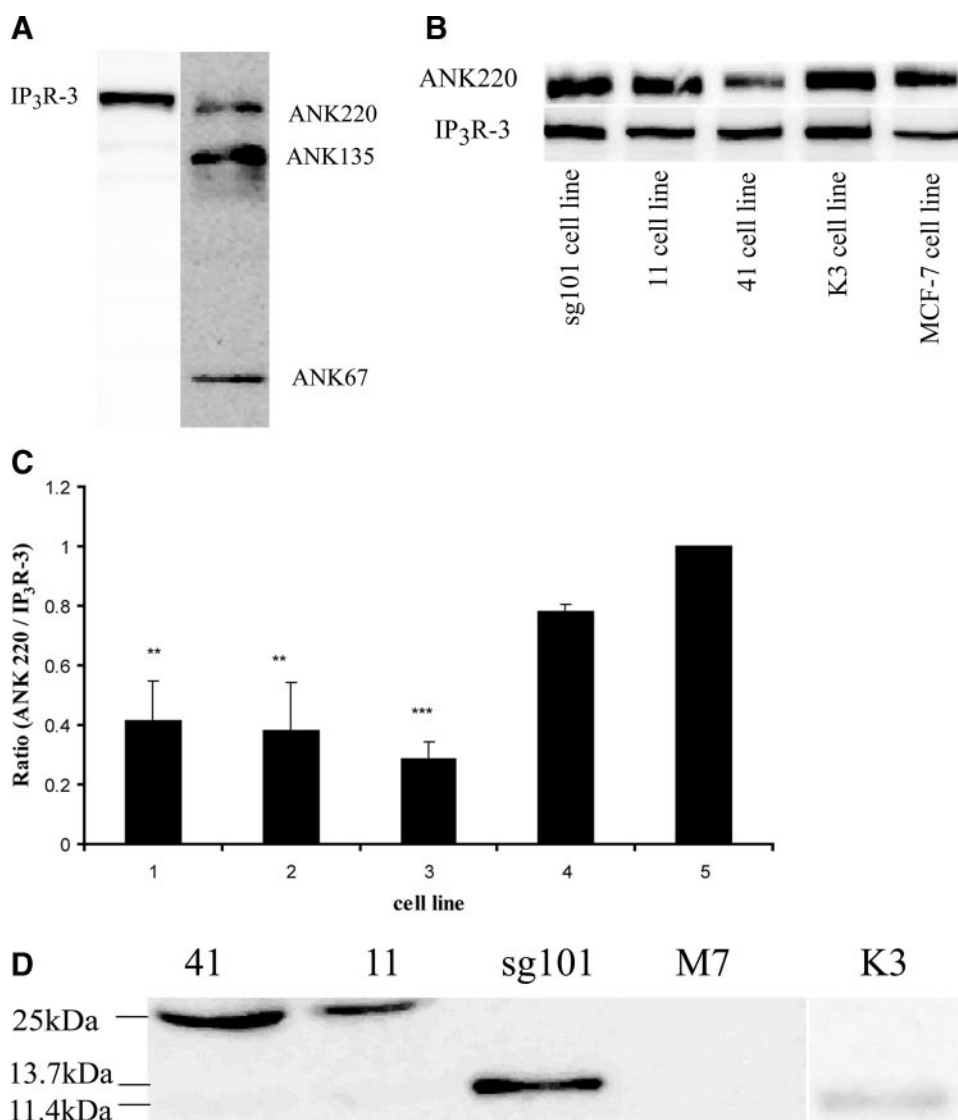


FIGURE 9. Immunoprecipitation of IP₃R-3 and ankyrin B in the five cell lines and analysis of complex content. A, identification of IP₃R-3 and ankyrin B in MCF-7 cells. MCF-7 cells (untransfected) were extracted and subjected to SDS-PAGE and Western blotting as described under "Experimental Procedures," using mouse anti-ankyrin B or mouse anti-IP₃R-3 antibodies. Visualization is by chemiluminescence. IP₃R-1 (IP₃R type 1) was not detected in separate experiments using anti-IP₃R-1 antibody (data not shown). B, immunoprecipitation of IP₃R-3 and ankyrin B complexes. Untransfected MCF-7 cells and the lines expressing either wild-type or truncated sigma-1 receptors were cultured to about 90% confluency, lysed, and immunoprecipitated with anti-IP₃R-3 antibody as described under "Experimental Procedures." The immunoprecipitate was then subjected to SDS-PAGE and Western blotting using anti-ankyrin B and anti-IP₃R-3 antibodies. Actin was used as internal standard for normalization of loading (not shown), and bands were visualized by chemiluminescence. C, immunoblots (shown in B) were digitally scanned and densitometrically analyzed using a Kodak Image Station 2000R, to obtain relative optical density units. Data were then expressed as a *bar graph* of ratio of ankyrin B220 over IP₃R-3. Data shown are mean \pm S.E. from three separate determinations. Numbering corresponds to cell line order in B. Lines sg101, 11, and 41 all showed significantly lower ratios when compared with untransfected MCF-7 cells (M7), with $p = 0.0096$, 0.01 , 0.0067 , respectively. Line K3 showed a somewhat lower ratio, but was not significantly different from untransfected MCF-7 cells ($p = 0.0858$). Asterisks indicate a significant difference: * = $p < 0.05$; ** = $p < 0.01$; *** = $p < 0.0001$. D, extracts from the five cell lines were immunoprecipitated using anti-ankyrin B antibody and subjected to SDS-PAGE and Western blotting as described under "Experimental Procedures." The blots were probed with C-terminal directed anti-sigma-1 antibody (1:100 dilution) to detect intact sigma-1 receptor and the C-terminal fragment and the N-terminal directed anti-sigma-1 antibody (1:200 dilution) to detect the N-terminal fragment.

of the receptor. As shown in Fig. 6, the level of BDK sensitivity is the same as that in line 41. However, unlike the effect in line 41, the constitutive positive modulation of the BDK response is not sensitive to sigma ligands. Preincubation with (+)-pentazocine, BD1063, or their combination produced no signifi-

cant change in the BDK-stimulated rise in $[Ca^{2+}]_i$ relative to cells pretreated with no ligand. Thus the effect of sigma ligands on the BDK response in the sg101 cell line is the same as that in the untransfected MCF-7 cells, and it is consistent with the inability of the C-terminal fragment to bind $[^3H](+)$ -pentazocine (Fig. 4D and Tables 3 and 4). Altogether, the data show that the C-terminal segment of the sigma-1 receptor is fully capable of positively enhancing the BDK response and that this activity can be fully dissociated from agonist binding and ligand regulation.

Examination of Protein-Protein Interactions in Cell Lines Expressing Sigma-1 Receptor Constructs—Hayashi and Su (26) showed that the sigma-1 receptor forms a trimeric complex with ankyrin B and IP₃R type 3 in the endoplasmic reticulum of NG-108-15 neuroblastoma-glioma hybrid cells. Sigma-1 receptor agonists caused the dissociation of an ankyrin B isoform from IP₃R-3. The degree of sigma-1 ligand-induced dissociation of ANK 220 from IP₃R-3 correlated strongly with efficacy in potentiating the BDK-stimulated rise in $[Ca^{2+}]_i$. This was indicated by demonstrating that the complex immunoprecipitated with antibody against IP₃R-3 contained less ANK 220 when cells were treated with sigma-1 agonist (26). We therefore surmised that our MCF-7 cell lines with the constitutively sensitized BDK calcium response should have less ankyrin associated with the IP₃ receptor compared with those that are not sensitized. Fig. 9A shows a Western blot of cell extract from untransfected MCF-7 cells probed with antibodies against isoforms of ankyrin B and subtypes of IP₃ receptor. The figure shows that MCF-7 cells express ankyrin 220, ankyrin 135, and ankyrin 67. The cells also

express IP₃ receptor type 3 (IP₃R-3), whereas IP₃ receptor type 1 (IP₃R-1) was not detected.

Fig. 9, B and C, shows the results of immunoprecipitation experiments to determine the content of complexes in the four MCF-7 cell lines. Cell extracts were immunoprecipitated with

Sigma-1 Receptor C-terminal Segment Activates IP₃ Receptor

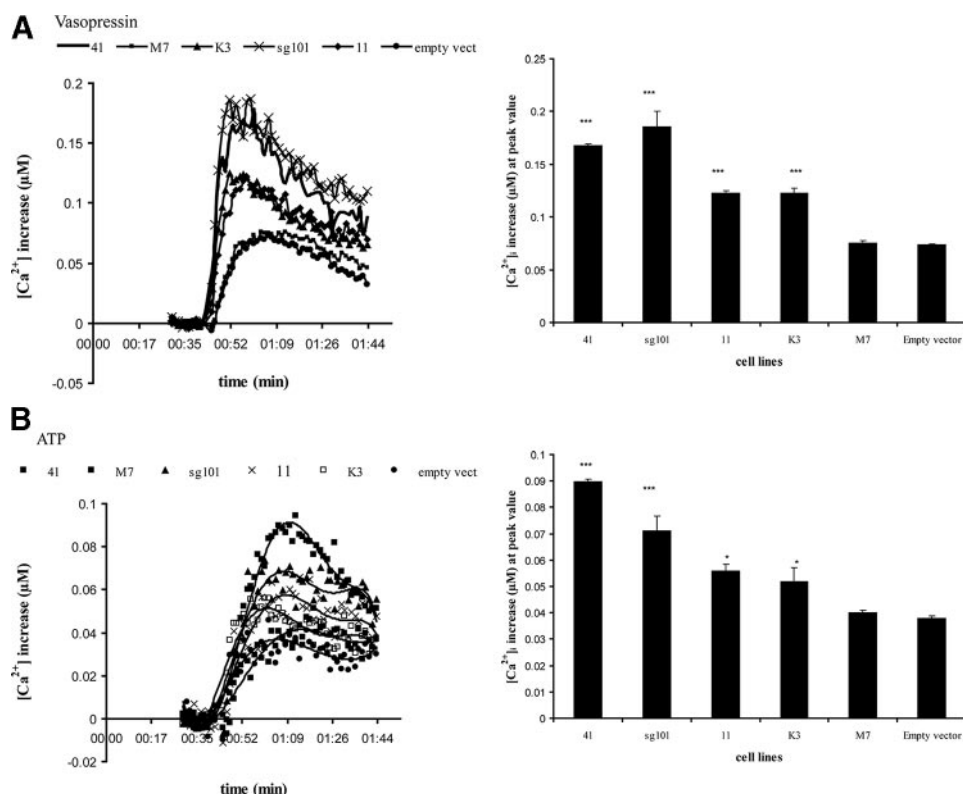


FIGURE 10. Effect of vasopressin and ATP on [Ca²⁺]_i in cell lines expressing the sigma-1 receptor and its truncated forms. The various cell lines were loaded with Fura-2 as described under "Experimental Procedures." After recording base line, vasopressin (final 800 nM) or ATP (final 50 μM) was rapidly injected, and [Ca²⁺]_i levels recorded and analyzed as described under "Experimental Procedures." For each panel, the graph on the left shows representative time versus [Ca²⁺]_i traces for each cell line, with all values normalized to base line. Each point is the averaged value from 6 wells. For clarity, the error bars have been removed. Standard error across the 6 wells was within 4.0–5.7%. Experiment was repeated six times. The graph on the right is a comparison of peak values from the time versus [Ca²⁺]_i traces shown as a bar graph, with each value representing the mean of peak [Ca²⁺]_i values from six separate experiments, ± S.E. Student's *t* test was used to analyze differences across cell lines relative to the untransfected control. *A*, vasopressin, 800 nM. ***, *p* < 0.001 for lines 41, 11, sg101, and K3; *p* = 0.9816 for empty vector transfected. *B*, ATP, 50 μM. ***, *p* < 0.0001 for lines 41 and sg101; *, *p* = 0.0317 and 0.0349 for lines 11 and K3, respectively; *p* = 1.021 for empty vector transfected.

antibodies against IP₃R-3, the immunoprecipitate subjected to SDS-PAGE and transferred. The blots were then subjected to Western analysis with antibodies against IP₃R-3 and ankyrin B. Fig. 9B shows that all the modified MCF-7 cell lines contained ANK 220 associated with IP₃R-3. Fig. 9C shows the ratio of ANK 220 to IP₃R-3 in the cell lines. The results show that lines 11, 41, and sg101 had a significantly lower ANK 220/IP₃R-3 ratio compared with lines K3 and untransfected MCF-7 cells. Furthermore, line K3 cells tended toward a lower ANK 220/IP₃R-3 ratio compared with untransfected cells, but the difference did not reach statistical significance.

The complexes were also analyzed for the presence of the sigma-1 receptor proteins. These results are shown in Fig. 9D. Cell extracts were immunoprecipitated with antibody against ankyrin B, and the immunoprecipitate was subjected to Western blot analysis using the antibodies described in Fig. 3 to detect the intact sigma-1 receptor (lines 41, 11, and M7), the C-terminal fragment (line sg101), and the N-terminal fragment (line K3). The results show that in lines 41 and 11, intact sigma-1 receptor is found present in the ANK 220-IP₃R-3 complex. In line sg101, the C-terminal fragment is found to be associated with the complex. Although present, very little N-terminal fragment is associated with the complex in line K3,

and no intact sigma-1 receptor is found in the complex from untransfected MCF-7 cells.

The profile of results shown in Fig. 9 correlates well with the degree of constitutive sensitization to BDK-stimulated calcium release across the cell lines as shown in Fig. 6. The cell lines expressing the wild-type sigma-1 receptor or its active C-terminal segment show a phenotypic decrease in the amount of ANK 220 associated with the IP₃ receptor, resulting in the constitutive enhancement of calcium release observed. Furthermore, the protein products of the expression constructs that give rise to constitutive enhancement (intact sigma-1 receptor and C-terminal fragment) are found to be associated with ankyrin B in the complex in these cells. In addition, the K3 cell line, which has lowest constitutive enhancement, has only a low amount of N-terminal fragment associated with the complex, whereas untransfected MCF-7 cells have no sigma-1 receptor in the complex, as expected. These results support the hypothesis that overexpression of the sigma-1 receptor drives the protein-protein interactions that result in IP₃ receptor activation and that the C-terminal segment of the receptor plays an important role in this process.

Effect of Sigma-1 Receptor Construct Overexpression on Other Phosphoinositide Agonists—Thus far, the effects of sigma-1 receptor overexpression have been demonstrated with only BDK. If the mechanism involves activation at the level of the IP₃ receptor, calcium release by other phosphoinositide agonists should also be constitutively enhanced. In addition to BDK receptors, MCF-7 cells also possess all subtypes of vasopressin receptors (V_{1a}, V_{1b}, and V₂) (39). V_{1a} and V_{1b} receptors are coupled to phosphoinositide turnover and intracellular calcium release, whereas V₂ receptors are coupled to cAMP formation. Fig. 10A shows that the rise in [Ca²⁺]_i stimulated by 800 nM vasopressin was enhanced in a nearly identical pattern as that of BDK-stimulated calcium release across the various cell lines (Fig. 6). Enhancement was highest in lines 41 and sg101, relative to untransfected cells or empty vector controls. Furthermore, both vasopressin and BDK showed intermediate augmentation in line K3 cells, with a level similar to that observed in line 11 cells.

MCF-7 cells have also been reported to express P2Y receptors for ATP, specifically the P2Y₂ subtype (40, 41). P2Y receptors are GPCRs coupled to phosphoinositide turnover and intracellular calcium release, whereas P2X receptors are ATP-

gated calcium channels (42). Fig. 10B shows the effect of 50 μ M ATP on $[Ca^{2+}]_i$ in the untransfected and transfected MCF-7 cell lines, with studies carried out in the absence of extracellular calcium to ensure measurement of release from intracellular stores only. ATP induced an increase of $[Ca^{2+}]_i$ in all cell lines, with a pattern across cell lines similar to that observed with BDK and vasopressin. These data taken together suggest that the constitutive enhancement of agonist-induced calcium release by overexpression of the sigma-1 receptor or its truncated C-terminal fragment may be universal across phosphoinositide-linked GPCR systems.

DISCUSSION

In this study, we set out to examine regions of the sigma-1 receptor that are involved in functional regulation of calcium signaling. We developed and analyzed MCF-7 cell lines that stably express the complete sigma-1 receptor or truncated N-terminal and C-terminal domains of the receptor. Cells expressing the wild-type receptor were designed to express at different levels to more readily quantitate the effect of overexpression. The functional end points examined were radioligand binding using $[^3H](+)$ -pentazocine, ability to modulate the bradykinin-stimulated increase in $[Ca^{2+}]_i$ in the absence and presence of sigma-1 receptor agonist and antagonist, and ability to alter the interaction of ankyrin B and IP₃R-3.

Western blot analysis showed that the cells expressed the expected protein products. Neither of the sigma-1 receptor fragments was as readily detectable at a 1:1000 dilution of the respective antibodies, relative to detection of the intact sigma-1 receptor. Because the commercial antibodies were raised against peptides found within the fragments, it is less likely that this is because of lower affinity of the antibody and more likely because of different levels of the proteins. The PCR data (Fig. 2) suggest comparable expression of message for the products in lines 41, K3, and sg101, with relatively lower expression in line 11. This may support the notion that the fragment proteins and intact receptor are initially expressed at comparable levels but that there is differential abundance of the protein products in the cells. Assuming that the antibodies have comparable affinities for fragments and intact protein, analysis of the data in Fig. 3 based on antibody dilutions would suggest that the relative level of N-terminal fragment in line K3 is somewhat higher than the level of C-terminal fragment in line sg101. Furthermore, the C-terminal fragment in line sg101 would appear to be in significantly lower abundance compared with the amount of intact sigma-1 protein found in lines 11 and 41, as indicated by the required lower dilution of the antibody for detection (Fig. 3, *A versus B*). A lower abundance of the fragments could result if they are not as stable in the cell as the intact sigma-1 protein.

As reported previously (7, 35, 36), MCF-7 cells did not show significant expression of typical sigma-1 receptors. However, they did express a low affinity binding site for $[^3H](+)$ -pentazocine, detectable only upon Scatchard analysis using high ligand concentrations, with $K_d = \sim 400$ nM (Table 3). The identity of this site is not known. It could represent the sigma-1 receptor splice variant that is reported to be undetectable using low concentrations of $[^3H](+)$ -pentazocine (36). This site will

be present as an endogenous site in all of the stably transfected cell lines.

It should be pointed out here that there are contrary reports of MCF-7 cells expressing sigma-1 receptors, as indicated by considerable levels of $[^3H](+)$ -pentazocine binding at low concentrations, RT-PCR, and/or Western blotting (43, 44). We have observed that highly passaged MCF-7 cells show significantly more $[^3H](+)$ -pentazocine binding compared with lower passage cells.⁴ We have also noted that at the more concentrated 1:100 dilution of the C-terminal directed antibody, a very faint band at 25 kDa can be detected in some batches of untransfected MCF-7 cells (data not shown) that cannot be detected at the 1:1000 dilution (Fig. 3A). Furthermore, although a two-site fit was not statistically better than a one-site fit, the Scatchard plot of $[^3H](+)$ -pentazocine binding to untransfected MCF-7 cell membranes shown in Fig. 4A has a slight biphasic nature, possibly suggesting detection of a very low number of endogenously expressed typical sigma-1 receptors in addition to the much more abundant low affinity site. These observations together could indicate that sigma-1 receptor expression may somehow be silenced in MCF-7 cells and that repeated passaging may relieve this silencing. This possibility needs further investigation, but it could account for the differences reported in the literature.

As expected, lines 11 and 41 expressed high levels of typical sigma-1 receptors as detected using $[^3H](+)$ -pentazocine. The single amino acid change of Kozak modification in line 41 did not affect binding activity, and the data confirmed higher expression compared with line 11 by 2-fold.

The N-terminal fragment expressed in line K3 exhibited only low affinity binding. Scatchard analysis revealed two low affinity binding sites. The first represents the endogenous site, whereas the second site represents the expressed construct. The level of expression could not be determined accurately by Scatchard analysis, because of the inability to saturate the site because of its low affinity. Because this construct also contains the Kozak modification, its expression level should be comparable with that of the wild-type receptor in line 41. However, as discussed above, other factors could affect its level in the cells. Nonetheless, despite the low affinity, significant $(+)$ -pentazocine binding to these membranes can occur (Table 4).

The C-terminal construct expressed in sg101 cells did not exhibit $[^3H](+)$ -pentazocine binding activity, even at high ligand concentrations (Fig. 4D and Table 4). Only the low affinity endogenous site is present in membranes from the sg101 cell line, suggesting lack of an agonist-binding site in the expressed C-terminal fragment. In the topology model proposed by Aydar *et al.* (27) (Fig. 1), the C-terminal fragment expressed in line sg101 would not have a transmembrane domain, possessing only a short hydrophobic helix that could provide some membrane anchorage. Thus, an initial concern was that this fragment may not be present in the membrane fractions and could be a cytosolic protein, accounting for the lack of $[^3H](+)$ -pentazocine binding to membranes. Membrane fractionation studies and salt wash

⁴ Z. Wu and W. D. Bowen, unpublished results.

Sigma-1 Receptor C-terminal Segment Activates IP₃ Receptor

experiments shown in Fig. 3D indicate that the C-terminal fragment protein is in fact predominantly associated with the ER membrane fraction, and to a lesser extent with the crude plasma membrane/mitochondrial (P2) fraction (not shown). However, it is not an integral protein, because it can be removed from the membrane with chaotropic salt washes. Interestingly, in untreated cells, a small amount of the protein is present in the cytosol, where it may or may not be functional. The data also support the models predicting a third site of membrane attachment in the intact sigma-1 receptor, in addition to the two predicted transmembrane helices.

Using site-directed mutagenesis, Yamamoto *et al.* (28) have shown that Ser-99, Tyr-103, Leu-105, and Leu-106 residues in the putative second transmembrane domain contribute strongly to agonist binding. Seth *et al.* (36) have shown by chemical modification that Asp-126 and Glu-172 residues in the C-terminal domain are critical for [³H]haloperidol binding. In addition, Pal *et al.* (45) have demonstrated that a fenpropimorph-like photoaffinity ligand is incorporated into both putative steroid binding domain-like (SBDL) regions of the sigma-1 receptor, which include aa 91–102 (SBDLI) and aa 176–194 (SBDLII). Therefore, it appears that high affinity ligand binding is the result of ligand interaction with residues contained in both the N-terminal and C-terminal segments of the sigma-1 receptor. This is consistent with the findings in this study, where there is a lack of high affinity binding to either the N-terminal or C-terminal constructs alone. Also, a previous study showed that the putative sigma-1 splice variant that lacks the third exon is nonfunctional in terms of binding agonist or antagonist, as demonstrated using [³H](+)-pentazocine, [³H](+)-PPP, and [³H]haloperidol (36). As pointed out above, the low affinity [³H](+)-pentazocine site found in untransfected cells could be the splice variant. The K3 construct has both the third and fourth exons deleted which would further decrease ligand binding ability.

We clearly show here that overexpression of the sigma-1 receptor in MCF-7 cells leads to a constitutive, positive modulation of BDK-stimulated calcium release. BDK stimulation of calcium release is substantially higher in line 11 and 41 cells compared with untransfected MCF-7 cells or cells transfected with empty vector (Fig. 6). This is apparent in the absence of sigma-1 agonist. The comparative level of constitutive enhancement is correlated with the level of sigma-1 receptor overexpression, with line 41 having about twice the level of sigma-1 receptor compared with line 11 and concomitantly showing twice the level of calcium enhancement.

Neither the sigma-1 agonist (+)-pentazocine nor the sigma-1 antagonist BD1063 had any effect on BDK stimulation in untransfected cells, consistent with the absence of sigma-1 receptors (Fig. 5). (+)-Pentazocine is able to augment BDK-stimulated calcium release in both line 11 and line 41 cells. Constitutive activation of the system is confirmed by the observation that the sigma-1 antagonist, BD1063, behaves as an inverse agonist, markedly inhibiting the response in both line 11 and 41 cells when added alone, with the effect being reversed by addition of (+)-pentazocine (Fig. 8, A and B). These results are in agreement with a report showing that co-expression of

sigma-1 receptors and Kv1.4 voltage-gated potassium channels in frog oocytes resulted in modulation of channel activity in the absence of sigma receptor ligands (27).

The cells expressing the sigma-1 receptor fragments exhibited differential BDK responses and sensitivities to sigma ligands. In line K3, expressing the N-terminal segment, a constitutive enhancement of the BDK response was observed, which was significantly less than that observed with cells expected to express a comparable amount of intact receptor (line 41 cells; see below) (Fig. 6). This modulation responded in an anomalous manner to sigma ligands, where both BD1063 and (+)-pentazocine inhibited the response (Fig. 8C). The ability to be regulated by sigma ligands is consistent with the demonstrated ability to bind (+)-pentazocine with low affinity. However, the loss of critical contact points present in the C-terminal region may change the way agonists and antagonists alter receptor conformation such that the receptor does not distinguish between the two, and both behave as inverse agonists.

The most striking finding was the observation that the sigma-1 receptor C-terminal segment, expressed in line sg101, is sufficient to give full enhancement of the BDK-stimulated increase in [Ca²⁺]_i, at a level equivalent to that in line 41 cells overexpressing the intact receptor (Fig. 6). Furthermore, the activity of the C-terminal construct is insensitive to modulation by either sigma-1 agonist or antagonist (Fig. 8D). Taken with the results from the line K3 cells, this indicates that the C-terminal region of the receptor contains the functional domain(s) necessary for the modulation of the IP₃ receptor. The lack of modulation by sigma ligands is consistent with the absence of [³H](+)-pentazocine binding activity in membranes from sg101 cells. The results also indicate that ligand regulatory activity of the sigma-1 receptor resides predominantly in the N-terminal segment of the receptor.

The mechanism by which sigma-1 receptors enhance ER calcium release upon co-stimulation of cells with BDK and a sigma-1 agonist has been shown to involve protein-protein interactions between the sigma-1 receptor, ankyrin isoforms, and the IP₃ receptor (26). In the presence of a sigma-1 agonist, the liganded sigma-1 receptor interacts with an ankyrin B-IP₃ receptor complex, causing dissociation of ankyrin from the IP₃ receptor and thereby relieving an inhibition imparted by the ankyrin. Several isoforms of ankyrin and IP₃ receptor exist. Although IP₃R-3 is coupled to both ankyrin B 220 and ankyrin B 135 in NG-108 cells, (+)-pentazocine appeared to predominantly dissociate ankyrin B 220 from IP₃R-3 and not ankyrin 135 (26). We show here that MCF-7 cells and its derived cell lines contain ankyrin B 67, 135, and 220 isoforms, as well as IP₃R-3 (Fig. 9A). Immunoprecipitation studies revealed that complexes precipitated with anti-IP₃R-3 antibodies from all the MCF-7 cell lines contain both IP₃R-3 and ankyrin B 220 (Fig. 9, B and C). However, the relative amount of ankyrin B 220 in the complex varied across the cell lines and was inversely proportional to the degree of constitutive activation of the BDK response observed. The ratio of ankyrin B 220 to IP₃R-3 was highest in the untransfected cells and lowest in line 41, 11, and sg101 cells. The ratio in line K3 cells was closest to that in untransfected cells. Furthermore, when the complex was pre-

cipitated with anti-ankyrin B antibody (Fig. 9D), the complexes from the most constitutively enhanced cells were found to contain considerable amounts of either intact sigma-1 receptor (lines 11 and 41) or C-terminal fragment (line sg101), whereas only a low amount of N-terminal fragment was found in complex from the moderately activated cell line (line K3). Because these data were obtained in the absence of sigma-1 receptor agonists, the results suggest that overexpressing the sigma-1 constructs drives the ankyrin B 220 interaction and causes the sensitized cell lines to phenotypically have a higher level of ankyrin-free, and thus more active, IP₃ receptor. The immunoprecipitation data also enforce the idea that it is the C-terminal region of the sigma-1 receptor that interacts with ankyrin B 220 to cause its dissociation from the IP₃R-3.

The results of the BDK dose-response curves across the cell lines (Fig. 7) show that the sigma-1 receptor-induced constitutive enhancement of calcium release is because of an apparent increase in the potency of BDK. Because it is unlikely that the sigma-1 receptor and the truncated constructs are having an effect on BDK receptor affinity, this could be due to an apparent increase in affinity of the IP₃R-3 for IP₃ that would result upon removal of ankyrin from IP₃R (24, 25). By this mechanism, any given amount of calcium could then be released with less IP₃ production.

Sigma-1 receptors and the truncated constructs were found to also constitutively regulate vasopressin- and ATP-stimulated calcium release with the same pattern across the cell lines observed with BDK (Fig. 10, A and B). It should be noted that in the presence of extracellular calcium, 50 μ M ATP produced a large rise in $[Ca^{2+}]_i$ that showed little difference across the various cell lines (data not shown). This observation suggests that in addition to P2Y₂ receptors, these cells may also contain P2X receptors (ATP-gated calcium channels) or that P2Y₂ receptor activation can subsequently stimulate extracellular calcium entry through channels. In any case, this extracellular component of the rise in $[Ca^{2+}]_i$ did not appear to be differentially regulated by sigma-1 receptors, lending specificity of the effect for intracellular calcium release.

The similarity in the effect of sigma-1 receptor overexpression for all three agonists is consistent with the site of action of the sigma-1 receptor being downstream from the specific GPCR being activated, exerting effects at the level of the IP₃ receptor. Thus, any agonist that stimulates phosphoinositide turnover and IP₃ production might be expected to show an enhanced calcium signal in cells overexpressing the active constructs.

There are some apparent discrepancies in the data that must be mentioned. The constitutive activation of the BDK response in line 11 is equivalent to that in line K3 (Fig. 6), and the same pattern is found with the other agonists (Fig. 10). If the C-terminal segment contains the functional domain, it seems inconsistent that the K3 construct would have a comparable level of activity to a cell line expressing the intact receptor. This discrepancy could possibly be explained by a differential level of expression in the two cell lines. The K3 construct contains the Kozak modification, whereas the line 11 construct for intact receptor does not. Thus, the level of expression of N-terminal fragment in line K3 is expected to be higher than that of intact

receptor in line 11 and more comparable with the expression of the intact receptor in line 41, which also has the Kozak modification. However, as mentioned above, the actual expression level of the N-terminal construct appears lower than expected, and its level relative to intact receptor in line 11 is difficult to assess. One might expect expression of the N-terminal construct to be reasonably high because [³H](+)-pentazocine binding is clearly detectable despite the very low affinity.

The behavior of line K3 relative to line 11 can be predicted from the respective BDK dose-response curves (Fig. 7). Although line 11 gives a full maximal response, only a partial maximal response is observed in line K3. On the other hand, the BDK ED₅₀ value is somewhat lower in the line K3 cells compared with line 11 cells (3.07 versus 12.1 nM). Also, whereas there is separation between the curves for line 41 and line K3 cells over the entire BDK dose range, with higher response in line 41, the BDK dose curves for line 11 and line K3 cells cross at around 30 nM. Below 30 nM the response is actually slightly higher in line K3 compared with 11. However, in the higher dose range the response is significantly higher in line 11, because of the reduced maximal response in line K3. Thus, although lines 11 and K3 appear to show comparable enhancement of the 60 nM BDK-induced calcium response in Fig. 6, close analysis of the full BDK dose-response curves reveals that overall the effect is reduced in line K3 relative to line 11, as would be consistent with the hypothesis. A similar explanation may also be in play with vasopressin and ATP.

Nonetheless, the fact that the N-terminal construct retains some ability to enhance the agonist-stimulated calcium response, show a small (although not statistically significant) degree of ankyrin dissociation, and has the ability to associate with the ankyrin B-IP₃ receptor complex suggests that it contains at least some structural features required for function. As shown in Fig. 9D, the N-terminal fragment is capable of interacting with the ankyrin-IP₃ receptor complex, but it may do so with low affinity as suggested by its low abundance in the complex compared with intact sigma-1 receptor and the C-terminal fragment. However, the N-terminal fragment that is present in the complex is capable of exerting an activating effect, as indicated by its ability to cause a leftward shift in the BDK dose curve that is comparable with the intact sigma-1 receptor and C-terminal fragment (Fig. 7). The decrease in maximal response to BDK shown with the N-terminal fragment is thus likely the reflection of the decreased amount of fragment in the complex. There may be residues in the C terminus of the N-terminal fragment (and therefore N-terminal to the sg101 construct) that also contribute to functional coupling.

Another apparent anomaly is the near equal constitutive enhancement of the calcium response in line 41 and line sg101 (Fig. 6). The level of intact sigma-1 receptor in line 41 should be much higher than the level of C-terminal fragment expressed in line sg101. First of all, the sigma-1 construct expressed in line 41 has the Kozak modification for high expression, whereas the C-terminal construct in line sg101 does not. As mentioned above, it is difficult to determine with accuracy the difference in protein expression level. However, comparing Fig. 3, A and B, it took a 10-fold less dilution of the antibody to detect the C-terminal fragment in sg101 compared with the intact receptor in

lines 41 and 11. Because the level of intact sigma-1 receptor in line 11 is half that of line 41, this suggests that the level of sigma-1 receptor in these cells is at least 10- and 20-fold higher, respectively, than the level of C-terminal fragment in line sg101. Therefore, in order for lines 41 and sg101 to have equivalent degrees of calcium enhancement, the C-terminal fragment would have to be much more active than the intact receptor in producing the constitutive response. The data in Fig. 9D may support this notion. More intact sigma-1 receptor is associated with the complex in line 41 cells compared with line 11 cells, consistent with the 2-fold higher receptor level and 2-fold higher activation in line 41. However, equivalent amounts of the C-terminal fragment appear to be associated with complex in sg101 cells compared with intact receptor in line 41 cells, despite the apparent lower abundance of C-terminal fragment, but consistent with the near equal activity observed in the two cell lines. It is interesting to speculate that in the intact receptor, the activity in the C-terminal segment is restrained in some way by the N-terminal segment. Agonist binding to the receptor may change the conformation such that the restraint is lifted and the C-terminal segment of the receptor can interact more avidly with the ankyrin B-IP₃ receptor complex. Thus, upon overexpression of the sigma-1 proteins, in the absence of agonist, more potent constitutive activation is observed with the unrestrained C-terminal fragment compared with the intact receptor.

In a recent report by Hayashi and Su (46) using Chinese hamster ovary cells, the sigma-1 receptor was shown to serve as a ligand- and calcium-sensitive chaperone protein in complex with BiP at the mitochondrion-associated ER membrane, where it regulates IP₃R-mediated calcium signaling into the mitochondrion. Experiments were carried out *in vitro* with purified glutathione S-transferase-fused sigma-1 receptor polypeptides. GST-sigma-1R-(116–223) was shown to have chaperone activity, blocking aggregation of denatured citrate synthase. However, GST-sigma-1R-(29–92) was inactive in this regard. Furthermore, GST-sigma-1R-(116–223) was found to complex with BiP *in vitro*. Therefore, the C-terminal polypeptide was most active as a chaperone partner. These findings are completely consistent with the *in vivo* findings reported herein with MCF-7 cells.

In conclusion, the findings presented here suggest that the sigma-1 receptor binds to ankyrin B 220 via its C-terminal region and causes dissociation from the IP₃ receptor. This results in sensitization of the cells to BDK-stimulated calcium release by increasing the amount of ankyrin-free IP₃R-3. The effect is pleiotropic, because transfected cells also become sensitized to the calcium response from vasopressin, ATP, and potentially other phosphoinositide-linked agonists. The ligand-induced regulation of this function appears to reside largely in the N-terminal region, although residues in the C terminus contribute to high affinity agonist binding. The ability to demonstrate differential functional effects of sigma-1 receptor constructs in stably transfected MCF-7 cells that originally are devoid of sigma-1 receptors suggests that the cell lines described here represent useful tools for exploring additional functions of sigma-1 receptors and the relationship of receptor structure to function.

Acknowledgments—We thank Drs. Tsung-Ping Su and Teruo Hayashi (NIDA, National Institutes of Health, and Department of Health and Human Services) for their initial gift of C-terminal and N-terminal directed anti-sigma-1 receptor antibodies, which allowed us to carry out some preliminary characterization of fragment expression. We acknowledge Matthew Dallos for completing some of the radioligand binding experiments as partial fulfillment of requirements for the Honors Degree in Neuroscience at Brown University. We also thank Dr. Enrique Cobos for optimizing some of the conditions for calcium measurement.

REFERENCES

- Sharkey, J., Glen, K. A., Wolfe, S., and Kuhar, M. J. (1988) *Eur. J. Pharmacol.* **149**, 171–174
- Su, T.-P., London, E. D., and Jaffe, J. H. (1988) *Science* **240**, 219–221
- Snyder, S. H., and Largent, B. L. (1989) *J. Neuropsychiatry Clin. Neurosci.* **1**, 7–15
- Quirion, R., Bowen, W. D., Itzhak, Y., Junien, J. L., Musacchio, J. M., Rothman, R. B., Su, T.-P., Tam, S. W., and Taylor, D. P. (1992) *Trends Pharmacol. Sci.* **13**, 85–86
- Bowen, W. D. (2000) *Pharm. Acta Helv.* **74**, 211–218
- Walker, J. M., Bowen, W. D., Walker, F. O., Matsumoto, R. R., de Costa, B. R., and Rice, K. C. (1990) *Pharmacol. Rev.* **42**, 355–402
- Vilner, B. J., John, C. S., and Bowen, W. D. (1995) *Cancer Res.* **55**, 408–413
- Hellewell, S. B., and Bowen, W. D. (1990) *Brain Res.* **527**, 244–253
- Hellewell, S. B., Bruce, A., Feinstein, G., Orringer, J., Williams, W., and Bowen, W. D. (1994) *Eur. J. Pharmacol.* **268**, 9–18
- Hanner, M., Moebius, F. F., Flandorfer, A., Knaus, H. G., Striessnig, J., Kempner E., and Glossmann, H. (1996) *Proc. Natl. Acad. Sci. U. S. A.* **93**, 8072–8077
- Clapham, D. E. (1995) *Cell* **80**, 259–268
- Simpson, P. B., Challiss, R. A., and Nahorski, S. R. (1995) *Trends Neurosci.* **18**, 299–306
- Berridge, M. J., Bootman, M. D., and Lipp, P. (1998) *Nature* **395**, 645–648
- McConkey, D. J., and Orrenius, S. (1996) *J. Leukocyte Biol.* **59**, 775–783
- Berridge, M. J. (1993) *Nature* **361**, 315–325
- Bezprozvanny, I. (2005) *Cell Calcium* **38**, 261–272
- Vilner, B. J., and Bowen, W. D. (1995) *Soc. Neurosci. Abstr.* **21**, 1608
- Vilner, B. J., and Bowen, W. D. (2000) *J. Pharmacol. Exp. Ther.* **292**, 900–911
- Zhang, H., and Cuevas, J. (2002) *J. Neurophysiol.* **87**, 2867–2879
- Brent, P. J., Herd, L., Saunders, H., Sim, A. T., and Dunkley, P. R. (1997) *J. Neurochem.* **68**, 2201–2211
- Ela, C., Barg, J., Vogel, Z., Hasin, Y., and Eilam, Y. (1994) *J. Pharmacol. Exp. Ther.* **269**, 1300–1309
- Bennett, V., and Baines, A. J. (2001) *Physiol. Rev.* **81**, 1353–1392
- Mohler, P. J., Schott, J. J., Gramolini, A. O., Dilly, K. W., Guatimosim, S., duBell, W. H., Song, L. S., Haurogne, K., Kyndt, F., Ali, M. E., Rogers, T. B., Lederer, W. J., Escande, D., Le Marec, H., and Bennett, V. (2003) *Nature* **421**, 634–639
- Bourguignon, L. Y., and Jin, H. (1995) *J. Biol. Chem.* **270**, 7257–7260
- Bourguignon, L. Y., Jin, H., Iida, N., Brandt, N. R., and Zhang, S. H. (1993) *J. Biol. Chem.* **268**, 7290–7297
- Hayashi, T., and Su, T.-P. (2001) *Proc. Natl. Acad. Sci. U. S. A.* **98**, 491–496
- Aydar, E., Palmer, C. P., Klyachko, V. A., and Jackson, M. B. (2002) *Neuron* **34**, 399–410
- Yamamoto, H., Miura, R., Yamamoto, T., Shinohara, K., Watanabe, M., Okuyama, S., Nakazato, A., and Nukada, T. (1999) *FEBS Lett.* **445**, 19–22
- Greco, S., Storelli, C., and Marsigliante, S. (2006) *J. Endocrinol.* **188**, 79–89
- Frey, B. M., Reber, B. F. X., Vishwanath, B. S., Escher, G., and Frey, F. J. (1999) *FASEB J.* **13**, 2235–2245
- Kozak, M. (1987) *Nucleic Acids Res.* **15**, 8125–8148
- Chirgwin, J. M., Przybyla, A. E., McDonald, R. J., and Rutter, W. J. (1979) *Biochemistry* **18**, 5294–5299

33. Bowen, W. D., de Costa, B. R., Hellewell, S. B., Walker, J. M., and Rice, K. C. (1993) *Mol. Neuropharmacol.* **3**, 117–126
34. Sazuka, T., Keta, S., Shiratake, K., Yamaki, S., and Shibata, D. (2004) *DNA Res.* **11**, 101–113
35. Seth, P., Fei, Y. J., Li, H. W., Huang, W., Leibach, F. H., and Ganapathy, V. (1998) *J. Neurochem.* **70**, 922–931
36. Seth, P., Ganapathy, M. E., Conway, S. J., Bridges, C. D., Smith, S. B., Casellas, P., and Ganapathy, V. (2001) *Biochim. Biophys. Acta* **1540**, 59–67
37. Ganapathy, M. E., Prasad, P. D., Huang, W., Seth, P., Leibach, F. H., and Ganapathy, V. (1999) *J. Pharmacol. Exp. Ther.* **289**, 251–260
38. Hayashi, T., Maurice, T., and Su, T. P., (2000) *J. Pharmacol. Exp. Ther.* **293**, 788–798
39. North, W. G. Fay, M. J., and Du, J. (1999) *Peptides* **20**, 837–842
40. Dixon, C. J., Bowler, W. B., Fleetwood, P., Ginty, A. F., Gallagher, J. A., and Carron, J. A. (1997) *Br. J. Cancer* **75**, 34–39
41. Wagstaff, S. C., Bowler, W. B., Gallagher, J. A., and Hipskind, R. A. (2000) *Carcinogenesis* **21**, 2175–2181
42. Burnstock, G. (2007) *Cell. Mol. Life Sci.* **64**, 1471–1483
43. Spruce, B. A., Campbell, L. A., McTavish, N., Cooper, M. A., Appleyard, M. V., O'Neill, M., Howie, J., Samson, J., Watt, S., Murray, K., McLean D., Leslie, N. R., Safrany, S. T., Ferguson, M. J., Peters, J. A., Prescott, A. R., Box, G., Hayes, A., Nutley, B., Raynaud, F., Downes, C. P., Lambert, J. J., Thompson, A. M., and Eccles, S. (2004) *Cancer Res.* **64**, 4875–4886
44. Wang, B., Rouzier, R., Albarracin, C. T., Sahin, A., Wagner, P., Yang, Y., Smith, T. L., Meric-Bernstam, F., Marcelo Aldaz, C., Hortobagyi, G. N., and Puzstai, L. (2004) *Breast Cancer Res. Treat.* **87**, 205–214
45. Pal, A., Hajipour, A. R., Fontanilla, D., Ramachandran, S., Chu, U. B., Mavlyutov, T., and Ruoho, A. E. (2007) *Mol. Pharmacol.* **72**, 921–933
46. Hayashi, T., and Su, T.-P. (2007) *Cell* **131**, 596–610